

PAPER • **OPEN ACCESS**

First passage and first hitting times of Lévy flights and Lévy walks

To cite this article: Vladimir V Palyulin *et al* 2019 *New J. Phys.* **21** 103028

View the [article online](#) for updates and enhancements.



PAPER

First passage and first hitting times of Lévy flights and Lévy walks

Vladimir V Palyulin¹ , George Blackburn^{2,3}, Michael A Lomholt⁴, Nicholas W Watkins^{3,5,6,7},
Ralf Metzler⁵ , Rainer Klages^{2,8,9}  and Aleksei V Chechkin^{5,10}¹ Centre for Computational and Data-Intensive Science and Engineering, Skolkovo Institute of Science and Technology, Nobelya Ulitsa 3, Moscow, 121205, Russia² Max Planck Institute for the Physics of Complex Systems, Nöthnitzer Straße 38, D-01187, Dresden, Germany³ Centre for Fusion, Space and Astrophysics, University of Warwick, Coventry, United Kingdom⁴ MEMPHYS—Centre for Biomembrane Physics, Department of Physics, Chemistry, and Pharmacy, University of Southern Denmark, DK-5230, Odense M, Denmark⁵ Institute for Physics & Astronomy, University of Potsdam, D-14476 Potsdam-Golm, Germany⁶ Centre for the Analysis of Time Series, London School of Economics and Political Sciences, London, United Kingdom⁷ Faculty of Science, Technology, Engineering and Mathematics, Open University, Milton Keynes, United Kingdom⁸ Institut für Theoretische Physik, Technische Universität Berlin, Hardenbergstraße 36, D-10623, Berlin, Germany⁹ Queen Mary University of London, School of Mathematical Sciences, Mile End Road, London E1 4NS, United Kingdom¹⁰ Akhiezer Institute for Theoretical Physics National Science Centre ‘Kharkov Institute of Physics and Technology’, Kharkov 61108, UkraineE-mail: chechkin@uni-potsdam.de**Keywords:** Lévy flights, Lévy walks, first-passage time, first-hitting timeRECEIVED
26 April 2019REVISED
23 August 2019ACCEPTED FOR PUBLICATION
5 September 2019PUBLISHED
11 October 2019Original content from this
work may be used under
the terms of the [Creative Commons Attribution 3.0 licence](https://creativecommons.org/licenses/by/4.0/).Any further distribution of
this work must maintain
attribution to the
author(s) and the title of
the work, journal citation
and DOI.

Abstract

For both Lévy flight and Lévy walk search processes we analyse the full distribution of first-passage and first-hitting (or first-arrival) times. These are, respectively, the times when the particle moves across a point at some given distance from its initial position for the first time, or when it lands at a given point for the first time. For Lévy motions with their propensity for long relocation events and thus the possibility to jump across a given point in space without actually hitting it (‘leapovers’), these two definitions lead to significantly different results. We study the first-passage and first-hitting time distributions as functions of the Lévy stable index, highlighting the different behaviour for the cases when the first absolute moment of the jump length distribution is finite or infinite. In particular we examine the limits of short and long times. Our results will find their application in the mathematical modelling of random search processes as well as computer algorithms.

1. Introduction

When a stochastic process $x(t)$ first reaches a given threshold value in many scenarios follow-up events are triggered: shares are sold when their value crosses a pre-set target amount, or chemical reactions occur when two reactive particles encounter each other in space. The time t at which this triggering event first occurs, is either called the first-hitting (first-arrival) or the first-passage time, as defined below [1–3]. While the physical analysis of first-passage time problems has a long history, notably the seminal works by Smoluchowski [4] as well as Collins and Kimball [5], even for the long-studied case of standard Brownian motion [6] significant progress has been achieved within the last decade [2, 7–9]. In particular, for finite domains interesting results were unveiled for the mean and global mean first passage times and their geometry-control [7, 10]. The often minute particle concentrations inside biological cells and the related concept of the few-encounter limit [11–13] motivated studies to obtain the full probability density function (PDF) of first-passage times in generic geometries, demonstrating strong defocusing (large spread of first-passage times) and an intricate interplay between geometry- and reaction-control [13, 14].

For non-Brownian stochastic processes additional complications in the determination of first-passage and first-hitting times arise. Conceptually, such *anomalous diffusion processes* are distinguished according to the value of the anomalous diffusion exponent ν in the long time limit of their mean squared displacement (MSD) $\langle x^2(t) \rangle = \int x^2 P(x, t) dx \simeq K_\nu t^\nu$, defined as ensemble average of x^2 over the particle PDF $P(x, t)$ [15–20]: the

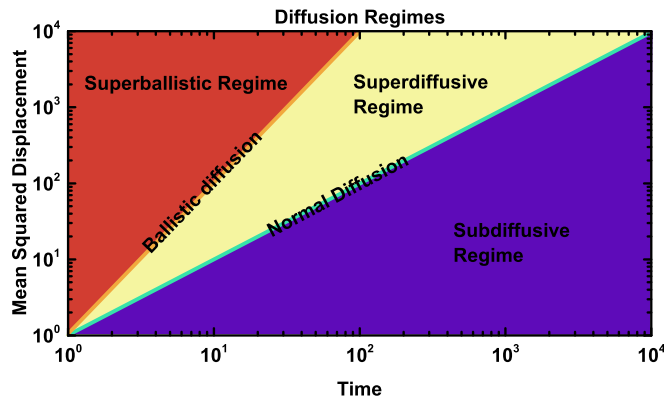


Figure 1. Anomalous diffusion regimes as characterised by the power-law scaling with time of the mean squared displacement (MSD). For normal diffusion the MSD grows linearly with time. However, other types of ‘anomalous diffusion’ are widely observed, for which the MSD grows as $\langle x^2(t) \rangle \simeq t^\nu$, where the anomalous diffusion exponent ν differs from unity. ‘Subdiffusion’ is slower than normal diffusion, corresponding to $\nu < 1$. Faster diffusion splits into the regimes of ‘superdiffusion’ with $1 < \nu < 2$, ‘ballistic motion’ with $\nu = 2$, and ‘superballistic’ with $\nu > 2$.

range $0 < \nu < 1$ corresponds to *subdiffusion* (or dispersive transport), while $1 < \nu < 2$ is referred to as *superdiffusion* (or enhanced transport). Beyond the regime $\nu = 2$ of ballistic transport, we encounter *superballistic motion*. Sometimes the range $3 < \nu < 5$ is called *hyperdiffusion* [21]. Examples for anomalous diffusion processes include turbulent flows [22], charge carrier transport in amorphous semiconductors [23], human travel [24], light waves in glassy material [25], biological cell migration [26–29], or transport of submicron tracer particles and fluorescently labelled molecules inside biological cells and their membranes [18, 30–32]. Figure 1 shows a schematic representation of the various regimes.

In anomalous diffusion the mentioned complications may arise due to long-ranged correlations, for instance, in the increments of Mandelbrot’s fractional Brownian motion [33], whose strongly non-Markovian character precludes the application of standard analytic methods to determine the first-passage dynamics [34–36]. Non-standard first-passage and first-hitting properties also arise for *Lévy flight* (LF) and *Lévy walk* (LW) processes, that are in the focus of this study. LWs and LFs are among the most prominent models for the description of superdiffusive processes [15–17, 20, 37–39]. Both models represent special cases of continuous time random walks [3, 40], in which relocation lengths are drawn from a long-tailed Lévy stable distribution with diverging variance. The difference between them is that LFs are Markovian processes in which jumps occur at typical time intervals. Therefore, the resulting LF process is characterised by a diverging MSD $\langle x^2(t) \rangle$ [3, 15, 40, 41]. LWs, in contrast, include a spatiotemporal coupling between jump lengths and waiting times, penalising long jumps with long waiting times, effectively introducing a finite velocity [42]. Jump lengths and waiting times may be coupled linearly, such that the resulting LW moves in a given direction with a constant speed until velocity reversal after a given waiting time, the velocity model [43], or the space-time coupling may have a power-law type [40]. The velocity may also be considered to change from one step to another [44, 45]. Interestingly, for certain parameters even Lévy walks have an infinite variance, namely, when there is a distribution of velocities associated with different path lengths [45]. LFs and LWs are non-ergodic in the sense that long time and ensemble averages of physical observables are different [19, 20, 45–49]. The linear response behaviour and time-averaged Einstein relation of LWs have been studied, as well [50, 51]. We note that LFs and LWs have also been formulated in heterogeneous environments [52, 53].

While for Brownian motion the events of first-passage and first-hitting (or first-arrival) are identical because space is being explored continuously [54], the possibility of long, non-local jumps lead to ‘leapovers’ [55, 56], single jumps in which a given point is overshoot by some leapover length, as illustrated in figure 2: for random walk processes with diverging variance of the jump length PDF, the event of first-passage becomes fundamentally different from that of first-hitting, and it is intuitively clear that first-hitting a target is harder (less likely) than the first-passage.

LFs and LWs have been studied for considerable time, however, the systematic comparison of some of their first passage properties started only recently [57]. We here systematically investigate the first-passage and first-hitting properties of LFs and LWs in one dimension by drawing generic conclusions on their differences and similarities. This is an important first step in the assessment of these two fundamental random search processes. Further applications of non-local, Lévy-type search are found in computer algorithms such as simulated annealing [58]. In higher dimensions the comparison is more complicated due to various possible definitions of LWs and LFs [59, 60]. In particular, so far studies of LFs and LWs mostly focused on the long-time features. However, in all search processes the short-time properties do contribute to the efficiency of the search [61], and

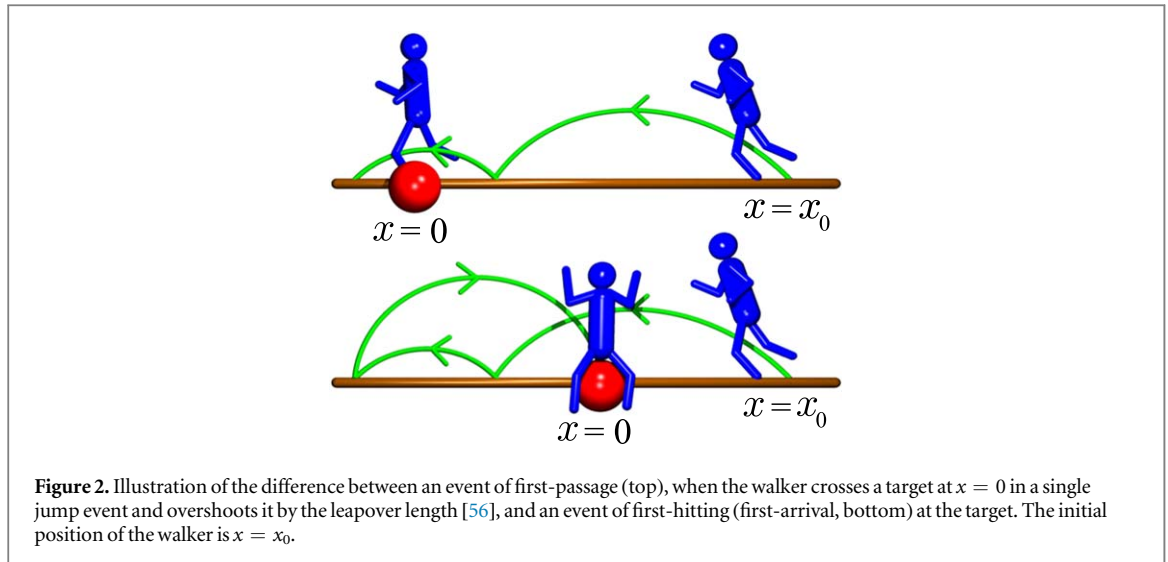


Figure 2. Illustration of the difference between an event of first-passage (top), when the walker crosses a target at $x = 0$ in a single jump event and overshoots it by the leapover length [56], and an event of first-hitting (first-arrival, bottom) at the target. The initial position of the walker is $x = x_0$.

in the light of the aforementioned scenarios of the few-encounter limit become even more relevant. We therefore pay considerable attention to the characteristics of the short-time first-passage and first-hitting properties of LFs and LWs.

Our paper is organised as follows. In section 2 we briefly review the rôle of LFs and LWs in random search processes, followed by setting the first-passage and first-hitting scenarios in section 3. Section 4 reports the first-passage properties of LFs and LWs, the first-hitting properties of both processes are then investigated in section 5. A summary and discussion is provided in section 6, and details of the mathematical derivations are deferred to the appendices.

2. The role of Lévy flights and walks in random target search

The term LF was coined by Benoît Mandelbrot in honour of his advisor, the French mathematician Paul Lévy, at École Polytechnique in Paris. In his famed treatise on the fractality of nature [62], Mandelbrot studied random walk processes with scale-free jump length distributions, leading to fractal trajectories of clusters of local motion interspersed with long relocations, on all scales.

As mentioned above LFs are Markovian and possess a diverging MSD. In that sense they are in most cases ‘unphysical’, as they appear to possess an infinite speed. While spatiotemporally coupled LWs provide a ‘non-pathological’ description with finite speed, LFs do have their justification in the following senses: first, when the process involves long-tailed jump lengths in some ‘chemical’ co-ordinate but local jumps in the physical, embedding space, the argument about a diverging MSD does not hold. An example is the random search of proteins on a DNA chain that is represented as a fast-folding chain in three dimensions [63]. Second, when we solely speak about the spatial trajectory described by the searcher yet are oblivious of the corresponding time trace, it is legitimate to speak of LFs. Third, the observed motion may be considered scale-free only within a limited range of relocation lengths, beyond which cutoffs may exist [64–66]. Fourth, we note that only very rarely have experimental foraging studies really tested for LWs [20, 67]. Fifth, in some physical systems the measured data indicate a divergence of the kinetic energy [68]. Finally, LWs represent a much harder mathematical problem than LFs while the LF assumption may already provide valuable insight into the system. For these reasons we study LFs and LWs in parallel, and we point out their commonalities and differences.

Interest in both LF and LW models in physics arose in the context of simple one-dimensional deterministic maps that generate superdiffusive motion encountered within the context of phase diffusion in Josephson junctions [69, 70]. It was then shown that diffusion in these maps could be understood in terms of LWs [43, 69–71]. Further motivation to investigate LFs and LWs was sparked by a remark of Michael Shlesinger and Joseph Klafter, that scale-free motion may present a more efficient means for exploring space in one and two dimensions as compared to Brownian motion [72]. The argument goes that while Brownian dynamics features repeated returns to already explored regions causing oversampling [3, 63], scale-free LFs and LWs, in contrast, avoid these returns and, hence, yield a more efficient search strategy¹¹.

¹¹ Note that many search processes indeed run off in effectively two dimensions (land-bound animals, birds or fish whose lateral motion has a much wider span than the vertical motion) or even one dimension (proteins searching a DNA, animals foraging in the border region between forests and grassland).

The high efficiency of Lévy search became famous when experimental data of the relocation distances of soaring albatross birds were reported to display long, power-law tails [73]. While this result was discussed controversially in the literature [74, 75], it prompted the proliferation of the *Lévy flight foraging hypothesis*. Roughly speaking, this hypothesis predicts that search processes with Lévy stable relocation length distributions provide an optimal search strategy by minimising the random search times under certain conditions, particularly for a low density of targets [67, 76, 77]. Although later many of the experimental studies testing the Lévy flight foraging hypothesis were found to contain experimental or methodological errors [20, 67, 78, 79], there exists ample evidence that many animals in fact do exhibit scale-free movements over a few orders of magnitude [77], or have at least a search component that is scale-free [75]. From a theoretical point of view, however, it was shown that even in the case of single-mode search LFs may not always optimise a suitably defined search efficiency [80, 81]. For example, if a target is located in the close vicinity of a starting point or the target lies ‘windward’ (in the direction of an external bias) from the searcher’s starting position, Brownian motion may outperform the search by LFs. Furthermore, depending on the precise biological and ecological conditions, often more complex search patterns, for instance, multimodal or intermittent search strategies, are superior to LFs and LWs [42, 61, 78, 82–86]. Generally, most of the intermittent and multimodal search strategies can be described as a combination of a local exploration mode and a scale-free (long relocation) mode [78, 87], where the frequent, long, relocations are described by Lévy motions [61, 82].

Interestingly, there exists a direct connection between the biological strategy of random search for targets and the mathematical problem of first-passage and first-hitting. In foraging theory one distinguishes between cruise and saltatory foragers. While in cruise search the forager looks out for targets during the movements, the forager is blind for its targets when moving for saltatory search, for which the searcher needs to land exactly on (or very close to) the target to actually detect it [80, 88]. A cruise forager searching for a single target, however, is modelled mathematically as a first-passage problem while saltatory search for a single target corresponds to a first-hitting problem. Solving these mathematical problems thus sheds light, at least in more simple, abstract settings, on specific aspects of biological foraging.

As a general rule first-hitting problems appear in most target search problems while first-passage relates to the crossing of thresholds. The latter problem has been studied for many decades in the context of Markovian processes (see, for instance [89]) and much initial work related to the Gaussian case. Classic applications of first-passage include vibration [90], sea states, and earthquakes [91]. The first-passage problem also appears in calculating the time to activation in cases like Gerstein’s and Mandelbrot’s model of neurons [92], and resonant activation [93]. Further motivation comes from applications of the area swept out by Brownian motion up to its first passage, where results can be heuristically motivated from first-passage theory scaling results [94]. Recent interest has included transitions from the bull-to-the-bear market in finance, extreme value statistics of temperature records [95], or the diffusion of atoms in a one-dimensional periodic potential [96] as well as problems of escaping an enemy territory. The existence of heavy-tailed log-price fluctuations in finance, modelled using α -stable processes in [97] has indeed been a strong initial motivation for the LF first passage problem.

3. Setup of the system: determining first-passage and first-hitting times

The problem of first-passage consists in the determination of boundary crossing dynamics of a searcher. In the general case first-passage properties can be studied for any kind of domains [1, 2, 10, 13, 14]. In this paper we consider the classical 1D setting. We are interested in the event when a searcher crosses the origin for the first time after initially being released at position $x_0 > 0$ (figure 2, upper part). For LFs the first-passage time corresponds to the moment in time when the searcher first hits a coordinate on the negative semi-axis. For LWs the first-passage time is defined as the time needed for a particle to reach the origin, that is, only the fraction of the last relocation event (from the arrival point of the previous relocation to crossing the origin) is included in the computation.

A first-hitting event occurs when the end point of a jump arrives exactly at the origin. In physics literature the first-hitting is often also called the first arrival [80, 98]. Here we will use the term hitting throughout the text to avoid possible ambiguities. Similar to the first-passage the event of first-hitting may be defined for a domain of any shape. Here we concentrate on point-like targets. Thus, in the case of LFs the first-hitting corresponds to an exact landing at the target coordinate. For LWs in our 1D scenario an event of first-hitting occurs when the last relocation ends at the target, that is, in the LW case this corresponds to a searcher who cannot identify the target while crossing it during the relocation event.

Our results are either derived from the fractional Fokker–Planck equation [15, 41, 52] or are obtained from simulations of the discrete Langevin equation

$$x_{n+1} - x_n = (K_\alpha \delta t)^{1/\alpha} \xi_\alpha(n) \quad (1)$$

for the searcher's position x_n , where $\xi_\alpha(n)$ is a set of random variables sampled from a symmetric Lévy stable distribution with the characteristic function $\exp(-|k|^\alpha)$. The time step is chosen as $\delta t = 0.001$ for LFs in all cases but those which required higher time resolution. In that case $\delta t = 0.0001$ was used (figure 10). While we keep the generalised diffusion coefficient K_α of dimension $\text{cm}^\alpha/\text{s}$ in our analytical results, we set it to unity in the numerical analyses. The noise $\xi_\alpha(n)$ was computed following the method described in [100]. For LFs the time dependence is then simply obtained by adding the time step δt to a counter at each jump. The set of landing points for LFs exactly corresponds to the set of end-of-relocation points for LWs and, hence, the same simulation procedure was used for both processes. For LWs, in turn, the parameter δt is not related to the time resolution any longer, but rather describes the width of the jump length distribution. We thus use $K_\alpha \delta t = 0.001$ for the first passage of LWs and $K_\alpha \delta t = 0.0005$ for the first hitting problem. In order to compute the time-dependent characteristics for LWs the durations of relocations were calculated from a given relocation length via the speed v_0 of the walk that we take as a constant value. In our simulation of LWs the direction at the beginning of each relocation event is changed with likelihood $\frac{1}{2}$ (that is, the searcher continues in the same direction with probability $\frac{1}{2}$), as the jump lengths are taken from the symmetric distribution of the ξ_α entries.

In all cases considered in this paper a searcher eventually crosses the boundary or finds the target with unit probability. Hence, the first-passage and first-hitting properties can be characterised by the properly normalised PDFs. We will denote them as $\varphi_{\text{PF}}(t)$ and $\varphi_{\text{PW}}(t)$ for the first-passage of LFs and LWs, respectively, and $\varphi_{\text{HF}}(t)$ and $\varphi_{\text{HW}}(t)$ for the first-hitting of LFs and LWs.

4. First-passage properties of Lévy flights and Lévy walks

In this section we focus on the first-passage dynamics of LFs and LWs. First we analyse the case of LFs. In the following subsection for LWs we compare the results with the LF case.

4.1. First-passage for Lévy flights

The first-passage of LFs, due to their Markovian character and the symmetric jump length distribution is necessarily characterised by the Sparre Andersen-scaling [1, 98] in the long time limit. The analytical expression for this limiting behaviour reads [56]¹²

$$\varphi_{\text{PF}}(t) \sim \frac{x_0^{\alpha/2}}{\alpha \sqrt{\pi K_\alpha} \Gamma(\alpha/2)} t^{-3/2}, \quad (2)$$

in terms of the initial position x_0 and the stable index α of the jump length PDF. Here and in the following, the symbol \sim denotes asymptotic equality, \simeq means asymptotically equal up to a prefactor (scaling equality), and \approx means approximately equal. Figure 3 illustrates that the simulations results (coloured squares) are in perfect agreement with the Sparre Andersen-scaling (2) shown by the black lines for α values that are smaller and larger than unity. Note the shift by constant factors between the different results.

Considering the corresponding short time behaviour in figure 4 one immediately realises that only for the case of Brownian motion ($\alpha = 2$) the PDF increases smoothly with time from the value zero at $t = 0$. For LFs with $\alpha < 2$ the first-hitting PDF exhibits a non-zero value at $t = 0$. For small α values (see the curve for $\alpha = 0.5$ in figure 4) the PDF decreases monotonically with time, while for larger α values an initial increase is observed, leading to a maximum beyond which the PDF crosses over to the long time Sparre Andersen-scaling. LFs with smaller α values have a higher propensity for long jumps, while for $\alpha \rightarrow 2$ the behaviour converges to the known Lévy–Smirnov law for Brownian motion. The abrupt increase of $\varphi(t)$ at $t = 0$ thus stems from LFs that directly overshoot the origin with their first jump away from their initial position x_0 . The associated probability p_{jump} can be estimated from the survival probability of the searcher (for the full derivation see appendix A),

$$p_{\text{jump}} \approx \frac{K_\alpha \sin(\pi\alpha/2) \Gamma(\alpha)}{\pi x_0^\alpha}. \quad (3)$$

For the α values considered in figure 4 we obtain the concrete values

$$p_{\text{jump}} \approx \begin{cases} \frac{K_{1/2}}{\sqrt{2\pi x_0}} \approx 0.178, & \alpha = \frac{1}{2} \\ \frac{K_1}{\pi x_0} \approx 0.064, & \alpha = 1, \\ \frac{K_{3/2}}{2\sqrt{2\pi x_0^3}} \approx 0.0178, & \alpha = \frac{3}{2} \end{cases} \quad (4)$$

where we used $x_0 = 5$ and $K_\alpha = 1$. These values are in perfect agreement with the simulations data in figure 4.

¹² Note that we here consider the long time limit at fixed initial position. For a discussion of the limiting behaviour in a more general setting, where x_0 may diverge, we refer the reader to [99].

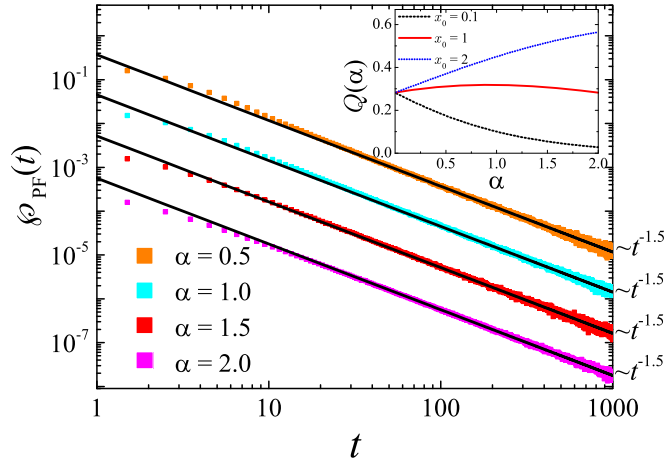


Figure 3. PDFs of first-passage times for LFs illustrating the universal Sparre Anderson-scaling (2) valid in the long time limit. Results for four different stable indices α are shown, as indicated in the graph. Simulations data (coloured squares) were obtained from $N = 10^7$ runs with initial position of the searcher $x_0 = 2$ and the generalised diffusion coefficient $K_\alpha = 1$. Black lines are obtained from equation (2). Note that for the better visual comparison of the PDFs to the exact asymptotic scaling, their values are divided by a factor of 10 for $\alpha = 1$, of 100 for $\alpha = 1.5$, and of 1000 for $\alpha = 2$. The inset shows the behaviour of the prefactor of the long-time dependence $\simeq t^{-3/2}$, $Q(\alpha) = x_0^{\alpha/2} / [\alpha \sqrt{\pi} K_\alpha \Gamma(\alpha/2)]$ from equation (2), for different x_0 and with $K_\alpha = 1$. Larger α values lead to more pronounced differences in the values of $Q(\alpha)$.

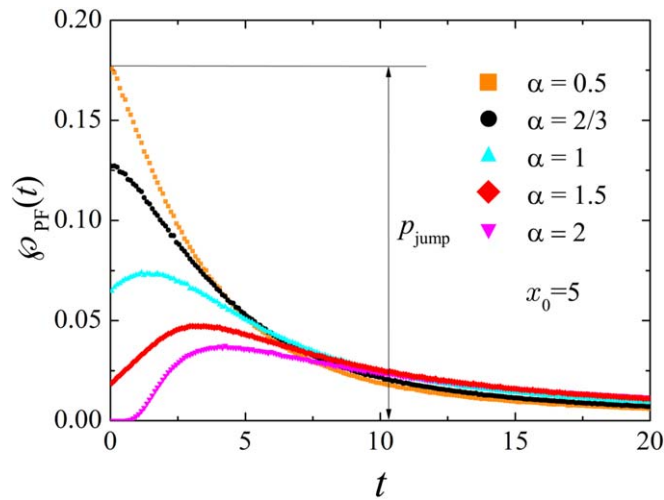
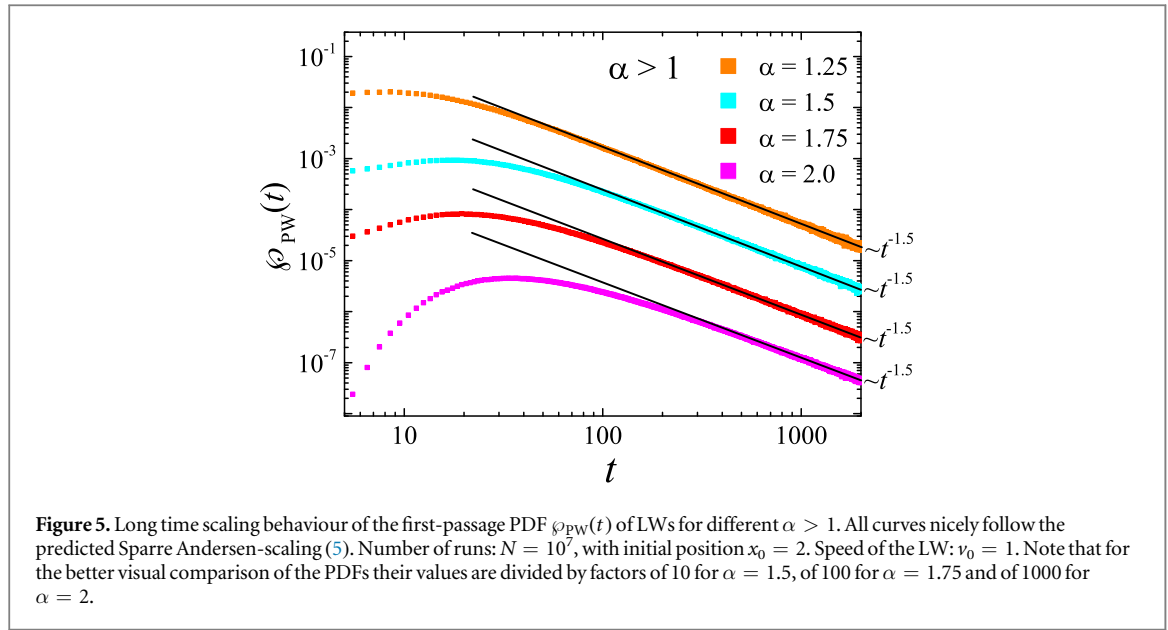


Figure 4. Short time behaviour of the first-passage time PDF for LFs, demonstrating that the change of the slope at $t = 0$ occurs for $\alpha = 2/3$ (for which we observe a horizontal tangent). Here p_{jump} is the probability that the boundary is immediately crossed with the first jump. Number of runs: $N = 10^7$, initial position: $x_0 = 5$, $K_\alpha = 1$.

Analytically one can also obtain the derivative of the PDF $\varphi_{PF}(t)$ for LFs in the short time limit (appendix A). It turns out that the monotonic decrease for small α values changes to the initial increase of the PDF at the value $\alpha = 2/3$, see figure 4. We note that in [101] the ‘limited space displacement’ of the trajectory corresponding to the Cauchy-Lorentz distribution for relatively low noise intensities at short times was discovered and analysed.

4.2. First-passage for Lévy walks

As laid out before, LWs spatiotemporally couple each relocation distance x with a time cost $t = x/v_0$. Nevertheless, starting from a Lévy stable jump length distribution, the points of visitation of an LW are identical with those of an LF with the same entries for the sequence of jumps—only the time counter for reaching the points of visitation differs for both processes. Hence, many properties of LWs can be understood from a subordination approach [102]: In some sense, to be specified below, an LW process can be considered as an LF with transformed durations of individual jumps. The PDF for the relocation times for LWs follows from the jump length PDF of LFs, as we show in appendix B. From the point of view of subordination one has to



discriminate the two cases $\alpha > 1$ and $\alpha \leq 1$. Namely, for $\alpha > 1$ the average duration of a jump is finite, and thus in the limit of a large number of jumps the time characteristics of LWs and LFs will only differ by a prefactor but should have the same scaling in time. From this scaling argument we expect the Sparre Andersen-scaling

$$\phi_{PW}(t) \simeq t^{-3/2}, \quad \alpha > 1 \quad (5)$$

to hold for the PDF $\phi_{PW}(t)$ of the first-passage of LWs, as long as $1 < \alpha \leq 2$. Indeed, the simulations results presented in figure 5 for 4 different values of α nicely corroborate the Sparre Andersen $t^{-3/2}$ scaling (5).

The problem of escape of LFs and LWs for $\alpha > 1$ was studied in [57]. The latter paper also proposes a formula for the effective diffusion coefficient for LWs expressed through the LW speed v_0 , the scaling factor σ_0 or the Lévy stable jump length PDF, and the stable index α (equation (55) in [57]). We derive this formula exactly in appendices B and C. Having an expression for the effective diffusion coefficient K_α^{LW} of LWs it seems pertinent to apply expression (2) to the LW dynamics. However, the numerical values obtained in this vein do not coincide with the simulation results. The values from the analytical results underestimate the simulations data in the limit of long t . This discrepancy is caused by the differences in the *short-time behaviour* between LFs and LWs. Namely, until the front of an LW reaches the boundary, the PDF of first-passage has a strictly zero value, due to the finite propagation front of LWs [20]. Modelling LWs by a rescaled LF process obviously neglects this important short-time feature. Hence a model LF process will exceed the real LW PDF at short times and, for reasons of normalisation, underestimate the PDF $\phi_{PW}(t)$ at long times.

For LWs with $\alpha \leq 1$ the observed long-time scaling deviates from the Sparre Andersen-scaling, as evidenced by the simulations data shown in figure 6. The fitted scaling exponents are consistent with the long time scaling

$$\phi_{PW}(t) \simeq t^{-\alpha/2-1}, \quad \alpha \leq 1 \quad (6)$$

considered in [103] which can also be rationalised in subordination terms. Indeed, the survival probability of an LF in the case of a first-passage scenario is inversely proportional to the square root of the number n of flights, that is, $\mathcal{S}_{LF}(n) \simeq n^{-1/2}$. For $\alpha < 1$ the number of jumps scales like $n \simeq t^\alpha$, such that $\mathcal{S}_{LF}(t) \sim t^{-\alpha/2}$. This scaling is equivalent to that obtained from the subdiffusive fractional diffusion equation [104]. Since the first-passage time PDF is the negative of the first derivative of the survival probability, we get $\phi_{PW}(t) \simeq t^{-\alpha/2-1}$. A strict derivation of this exponent for LWs can be found in [105], where the general result for $\phi_{PW}(s)$ is shown to be a function of the step length distribution in Laplace space. This general expression produces both the Sparre Andersen-scaling for $\alpha > 1$ and the exponent $-1 - \alpha/2$ for $\alpha < 1$.

The short-time limit of the first-passage time PDFs of LWs shown in figures 7 and 8 is noticeably different from the behaviour of LFs (compare figure 4). Namely, for LWs the spatial spreading is limited by a front which travels with the constant speed v_0 , while for the LF case the PDF $\phi_{PF}(t)$ has non-zero values at any non-zero time. Before the front of an LW reaches the origin the PDF of first-passage times is identically zero. At exactly $t = x_0/v_0$ we observe a jump in the value of the first-passage PDF. This jump corresponds to all those walkers which did not change the direction even once since the process started. Then, similarly to LFs, the function decays monotonically for small α or has an intermediate maximum.

We notice that in the limit $\alpha = 2$ of Gaussian relocations the resulting motion performed with a constant speed is similar to the model of immortal creepers [106]. For this type of motion the first-passage behaviour was

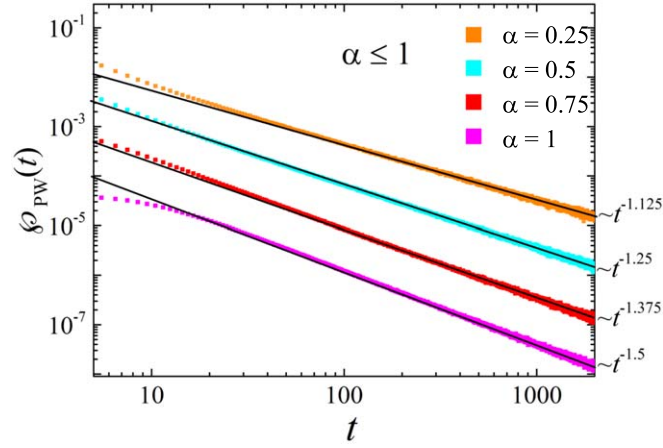


Figure 6. Long time scaling of the first-passage PDF $\varphi_{PW}(t)$ of LWs for different $\alpha \leq 1$. The fitted scaling exponents are in nice agreement with the prediction of equation (6). The results are obtained from $N = 10^7$ runs with initial position $x_0 = 2$, and relocation speed $v_0 = 1$. Note that for the better visual comparison of the PDFs their values are divided by a factor of 10 for $\alpha = 0.5$, of 100 for $\alpha = 0.75$ and of 1000 for $\alpha = 1$.

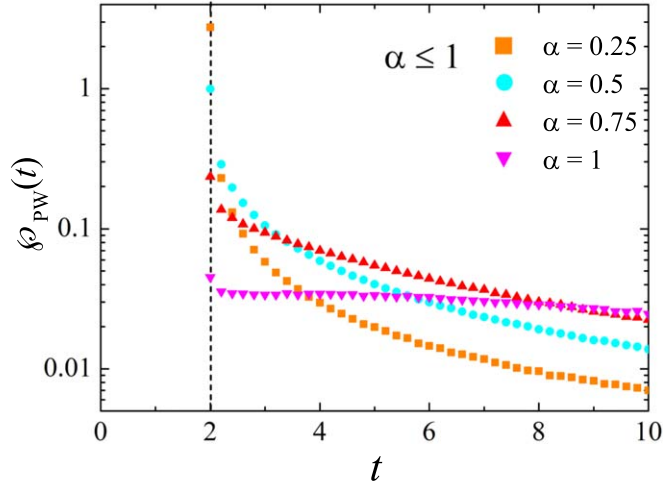


Figure 7. Short-time behaviour of the first-passage PDF of LWs for different $\alpha \leq 1$. The results are averaged over $N = 10^7$ runs with initial position was $x_0 = 2$ and LW speed $v_0 = 1$.

studied. However, in the model considered in [106] the creepers change direction with a waiting time PDF $\psi_{\text{creeper}}(t) = \omega e^{-\omega t}$, where ω is the characteristic turning frequency. In our case one has to compute the distribution of relocation times from the Gaussian characteristic function of the process. For $\alpha = 2$ in our case (compare appendix B),

$$\psi(\tau) = \frac{1}{\sqrt{\pi}} \frac{v_0}{\sigma_0} \exp\left(-\frac{v_0^2 \tau^2}{4\sigma_0^2}\right), \quad \langle \tau \rangle = \frac{2\sigma_0}{v_0 \sqrt{\pi}}. \quad (7)$$

Hence the equation (56) for the survival probability derived in [106] is not directly applicable in our case.

Generally, the jump of $\varphi_{PW}(t)$ occurs at the very moment when the propagation front, the fraction of particles having moved the distance vt without direction changes, passes through the boundary. This front corresponds to a delta peak with decreasing amplitude, moving with the wave variable $|x| \pm v_0 t$ (appendix D). Formally, that is, the value of the PDF at the time when this peak reaches the boundary is infinite, $\varphi_{PW}(t_0 = x_0/v_0) \rightarrow \infty$, as the survival probability changes as a step function¹³. In the simulations the PDF values are obtained from collecting crossing events in finite bins whose size represents the time resolution. Hence, the finite numerical values at t_0 are an artefact of the binning, and a finer mesh will produce larger values

¹³ The prefactor of the δ -function can be computed analytically as shown in appendix D.

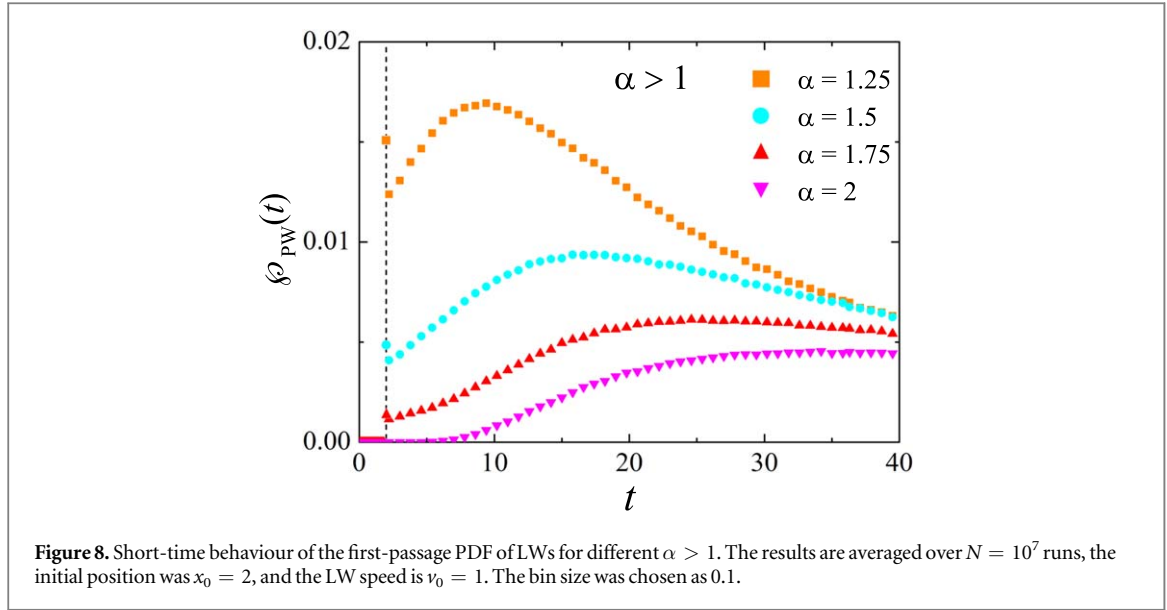


Table 1. Values of the LW first passage $\wp_{PW}(t)$ at $t = 2$ for two different α values and different bin sizes.

Bin size	$\alpha = 0.5$	$\alpha = 1.5$
10^{-1}	0.998	0.0049
10^{-2}	3.232	0.0011
10^{-3}	10.52	0.0075
10^{-4}	35.16	0.718

of $\wp_{PW}(t)$ (at $t = 2$ for the simulations parameters used for figure 8). We verified that this is indeed the case, as demonstrated by table 1.

The difference in behaviour of the first-passage PDF between the cases $\alpha \leq 1$ and $\alpha > 1$ as shown in figures 7 and 8 can be explained by the difference in the shape of the LW propagators (compare figure H1). In fact, for $\alpha > 1$ the position PDF of LWs has a front (smaller spikes in figure H1) producing the jump in the first-passage PDF, then the main, bell-shaped part of the PDF arrives, and the first-passage PDF grows gradually. For $\alpha < 1$, in contrast, the fronts are the only maxima in the position PDF, and thus the PDF of first-passage has a non-zero value and then decays monotonically.

5. First-hitting properties of Lévy flights and Lévy walks

In order to observe first-hitting events in a one-dimensional setting, we necessarily need to require that the first absolute moment $\langle |x| \rangle$ of the jump length PDF exists, corresponding to the requirement $\alpha > 1$ [61, 81]. For the opposite case of $0 < \alpha < 1$ the associated first-hitting time PDF vanished identically to zero. We do not consider the latter case here. For LWs an event of first-hitting in our setting occurs when the end point of a relocation with speed v_0 hits the target.

5.1. First-hitting properties of Lévy flights with $\alpha > 1$

The probability of first-hitting (see figure 2) clearly depends on the exact target size [107]. Here we will concentrate on the case of point-like targets. Detailed studies of the first-hitting properties of LFs were presented in [80, 81, 98]. Analytical derivations are based on the fractional Fokker–Planck equation [15, 52] with a sink term,

$$\frac{\partial f(x, t)}{\partial t} = K_\alpha \frac{\partial^\alpha f(x, t)}{\partial |x|^\alpha} - \wp_{HF}(t) \delta(x), \quad (8)$$

where the fractional derivative is defined in terms of its Fourier transform, $\int_{-\infty}^{\infty} \exp(ikx) [\partial^\alpha f(x, t) / \partial |x|^\alpha] dx = -|k|^\alpha f(k, t)$, where $f(k, t)$ is the Fourier transform of $f(x, t)$. Equation (8) can be easily modified to include an

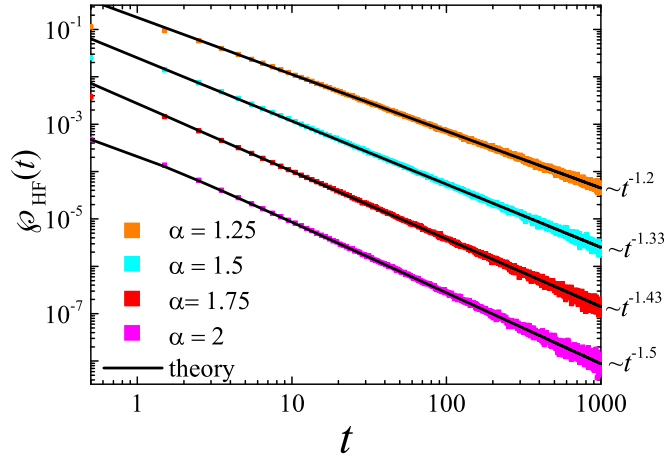


Figure 9. First-hitting time PDF for LFs with different α illustrating the long time scaling law (12), here represented by the black lines with slopes predicted by the analytical expression. The coloured symbols depict the simulations results. Note that for better visual comparison the PDFs are divided by a factor of 10 for $\alpha = 1.5$, of 100 for $\alpha = 1.75$, and of 1000 for $\alpha = 2$. We chose $K_\alpha = 1$.

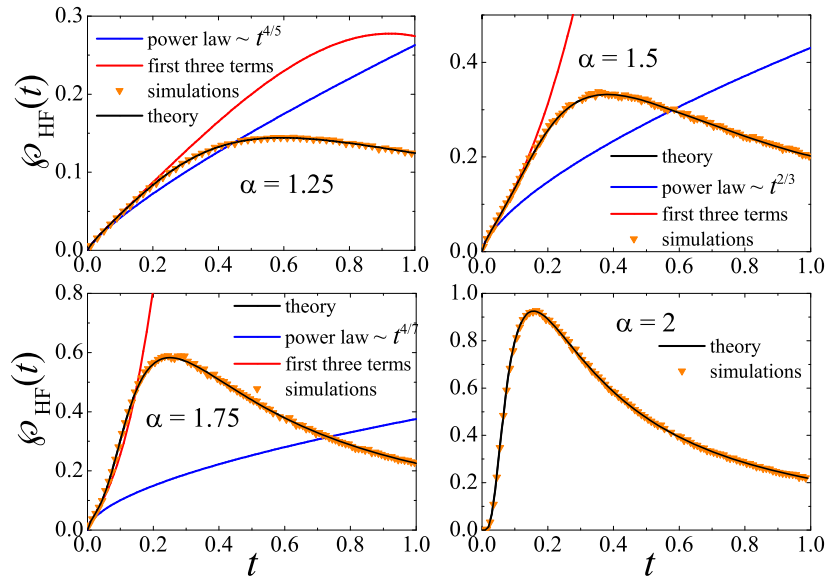


Figure 10. Short-time asymptotic for the first-hitting time PDF of LFs. The black lines are computed from the full expression (10), the blue lines show the power-law (13) with the exact prefactor as given by the first term in expansion (F.2), equation (F.4). The red lines show the sum of the first three terms of the expansion, combining equations (F.4), (F.5), and (F.6). Parameters: $K_\alpha = 1$ and $x_0 = 1$.

external drift [81], to the case of multiple point-like targets [82], or to include an additional Brownian or Lévy component with different stable index α' [61, 82]. We consider here a perfectly absorbing sink. The case of a finite absorption strength can be found in [108]. Equation (8) can be solved in Laplace space for the initial condition $f(x, 0) = \delta(x - x_0)$ [98], yielding

$$\varphi_{\text{HF}}(s) = \frac{\int_{-\infty}^{\infty} dk \frac{e^{ikx_0}}{s + K_\alpha |k|^\alpha}}{\int_{-\infty}^{\infty} dk \frac{1}{s + K_\alpha |k|^\alpha}}. \quad (9)$$

From inverse Laplace transform of this expression we obtain a new result for the first-hitting time PDF in time (see appendix E),

$$\varphi_{\text{HF}}(t) = \frac{\alpha \sin(\pi/\alpha) K_\alpha^{1/\alpha}}{\pi} t^{1/\alpha-1} \int_0^\infty dk \cos(kx_0) E_{1,1/\alpha}(-K_\alpha k^\alpha t), \quad (10)$$

where $E_{1,1/\alpha}(-K_\alpha k^\alpha t)$ is a two-parameter Mittag-Leffler function, which can be defined by its series expansions [109]

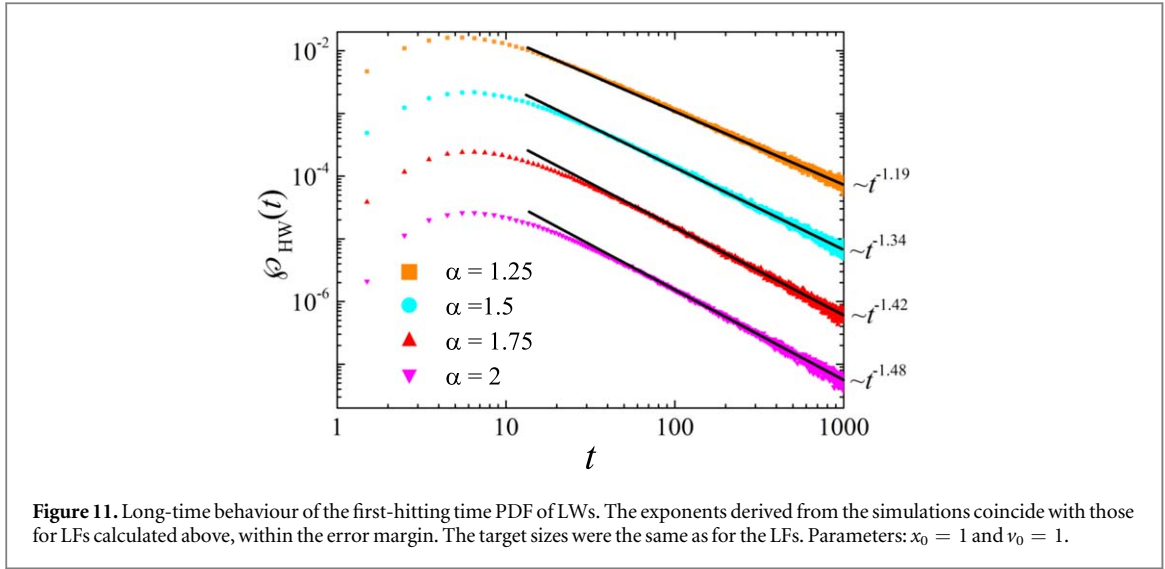


Figure 11. Long-time behaviour of the first-hitting time PDF of LWs. The exponents derived from the simulations coincide with those for LF's calculated above, within the error margin. The target sizes were the same as for the LF's. Parameters: $x_0 = 1$ and $v_0 = 1$.

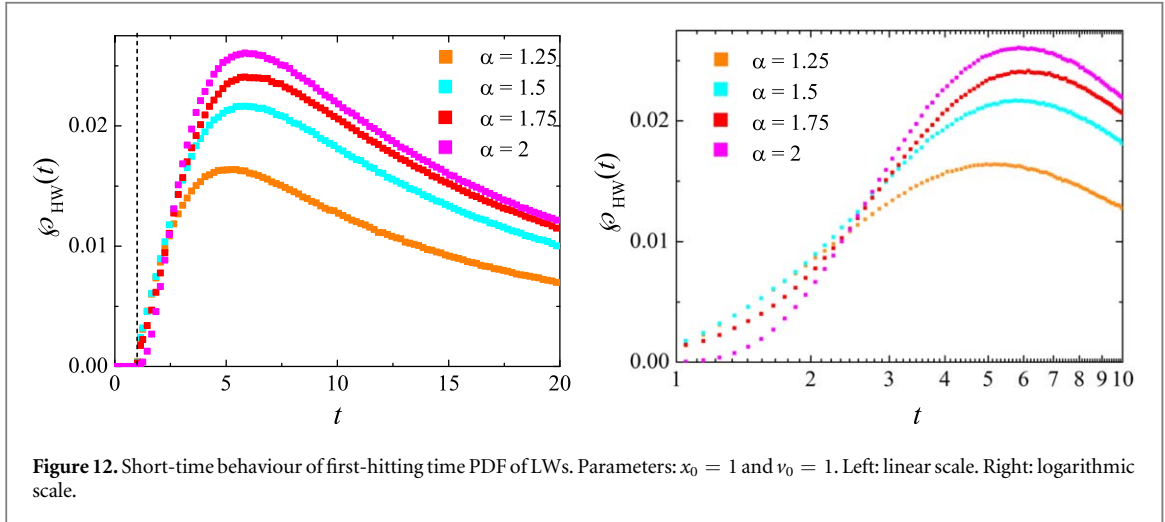


Figure 12. Short-time behaviour of first-hitting time PDF of LWs. Parameters: $x_0 = 1$ and $v_0 = 1$. Left: linear scale. Right: logarithmic scale.

$$E_{\alpha,\beta}(-z) = \sum_{k=0}^{\infty} \frac{(-z)^k}{\Gamma(\beta + \alpha k)} \sim \sum_{k=1}^{\infty} \frac{(-1)^{k+1}}{z^k \Gamma(\beta - \alpha k)}, \quad z > 0 \quad (11)$$

around zero and infinity, respectively. From the latter expansion we immediately recover the well-established power law asymptotic for the first-hitting time PDF of LF's [98],

$$\phi_{\text{HF}}(t) \simeq t^{1/\alpha-2} \quad (12)$$

at long times (compare equation (E.7) and its derivation in appendix E). We here also derive the short time scaling law

$$\phi_{\text{HF}}(t) \simeq t^{1/\alpha} \quad (13)$$

in appendix F. The full expression (10) can be evaluated numerically to plot the analytical solution of (8).

To determine the first-hitting time PDF from simulations of a searcher jumping according to a Lévy stable jump length distribution, we need to endow the target with a finite size d . This size needs to be large enough to guarantee sufficiently many events for proper statistics, however, it should be small enough to vouchsafe the point-like character of the target and thus warrant consistency with equation (8). This correct size also depends on the time resolution and the time cutoff of the simulation run but not on the number of runs (see appendix G). As a criterion for the choice of the target size we checked agreement with both the expected long-time power law (12) and the short-time power law (13). We found that for the integration time step $\delta t = 0.001$ and the time limit 10^3 for every run the proper target sizes are $d = 0.06$ for $\alpha = 2$ (Brownian motion), $d = 0.035$ for

Table 2. Comparison of the long-time asymptotes of the first-passage and first-hitting PDFs for LFs and LWs.

	First-passage	First-hitting
Brownian motion	$\wp_{\text{PBM}}(t) = \wp_{\text{HBM}}(t) = \frac{x_0}{\sqrt{4\pi K_2 t^3}} \exp\left(-\frac{x_0^2}{4K_2 t}\right)$	
Brownian creepers	$\wp_{\text{PBC}}(t) \simeq t^{-3/2}$	$\wp_{\text{HBC}}(t) \simeq t^{-3/2}$
Lévy flights ($1 < \alpha < 2$)	$\wp_{\text{PF}}(t) \simeq t^{-3/2}$	$\wp_{\text{HF}}(t) \simeq t^{1/\alpha-2}$
Lévy flights ($\alpha \leq 1$)	$\wp_{\text{PF}}(t) \simeq t^{-3/2}$	$\wp_{\text{HF}}(t) = 0$
Lévy walks ($1 < \alpha \leq 2$)	$\wp_{\text{PW}}(t) \simeq t^{-3/2}$	$\wp_{\text{HW}}(t) \simeq t^{1/\alpha-2}$
Lévy walks ($\alpha \leq 1$)	$\wp_{\text{PW}}(t) \simeq t^{1-\alpha/2}$	$\wp_{\text{HW}}(t) = 0$

$\alpha = 1.75$, $d = 0.014$ for $\alpha = 1.5$, and $d = 0.003$ for $\alpha = 1.25$. In particular we note here that this question of the finite target size is not limited to Lévy stable motion, but is also an issue for regular Brownian motion.

Figure 9 shows the long-time behaviour of the first-hitting time PDF for LFs. The PDFs obtained from simulations (coloured symbols) are well fitted by the theoretical result (E.7). In figure 10 we illustrate the corresponding short-time behaviour for the first-hitting time PDF. The black curves show the exact analytical solution computed from equation (10). Orange triangles are the simulation results. The correspondence between the analytical expression and the simulations is excellent. The blue curves correspond to the first term in the expansion (F.2) proportional to $t^{1/\alpha}$, which apparently works better for smaller α . For $\alpha = 2$ all coefficients in expansion (F.2) become equal to zero, that is, it does not work for the Brownian case. Generally, the terms of the expansion depend on time as $t^{k+1/\alpha}$ with k being the degree of the expansion. Once more terms of the expansion are added the quality of the approximation improves substantially (red curves in figure 10).

5.2. First-hitting probability for Lévy walks with $\alpha > 1$

In figure 11 we show the numerical data for this case in the limit of long times. The numerically determined scaling exponents nicely coincide with those obtained analytically and numerically for LFs (compare figure 9). The reason for this similarity is the same as for the case of first-passage: in the long time limit for $\alpha > 1$ both processes have the same scaling behaviour due to the existence of a finite scale of the jumps in the processes. The only difference is that the prefactors in both cases may differ, corresponding to a renormalisation of the mean step time.

Naturally, the short-time properties of the first-hitting behaviour depicted in figure 12 for LWs differ from the corresponding shape for LFs, in analogy to our observations for the first-passage case. Namely, no first-hitting event can occur before the LW front reaches the target. Then a jump in the value occurs at $t = x_0/v_0$. Similar to our discussion of the first-passage time PDF we attempted to insert an effective diffusion coefficient K_α^{LW} in the known long-time expressions for LFs, equation (E.7). Given that this did not succeed for the first-passage scenario, it is not surprising that an effective description in terms of LFs cannot approximate the LW behaviour.

6. Conclusions

LFs and LWs are broadly used models for efficient random search processes. In this paper we systematically analysed and compared the first-passage and first-hitting properties for two different models of Lévy motion, namely, LFs and LWs. We demonstrated that for $\alpha > 1$ the results of these two models are qualitatively identical at long times due to the finite average length of a relocation. The situation drastically changes for $\alpha < 1$ when the scaling of the PDFs heavily depends on the exact model (see the summary in table 2). This difference does not come as a surprise in view of the strong difference of the propagators of the two models, particularly, the finite propagation front of LWs. Nevertheless, having quantitative data for the associated first-passage and first-hitting time PDFs is valuable for any concrete analysis of search models based on LFs and LWs.

While our findings are consistent with the results for the escape from an interval established in [57], we observed that the exact short-time behaviour of LFs and LWs influences the whole first-passage and first-hitting time PDFs, and particularly alters the amplitude factor of the long-time scaling behaviour of LWs with an effective diffusion coefficient. In this short-time limit the PDF of the first-passage time of LFs jumps instantly to a finite value, which is not typical for the first-hitting of LFs. In the case of LWs the short time behaviour is defined by the passage of the propagation front through the boundary or the target. Strictly speaking the front passes instantly through any coordinate. Hence, the value of the PDF should be formally infinite at that instant. Obviously, this feature is smoothened in simulations and real observations due to finite binning, but it reveals

itself through a strong dependence of the value of the PDF at this instant on the time resolution of the simulations. In essence we showed that it is important to know the entire first-passage or first-hitting PDF in order to reach fully quantitative conclusions.

It will be interesting to extend the results reported herein to higher dimensions and/or multiple target scenarios. Higher-dimensional LFs and LWs can be defined in different ways [59, 60], and it is not *a priori* clear whether the difference in definitions modifies the behaviour for the first-passage and first-hitting time PDFs. In the case of multiple targets, for instance, disks distributed randomly in a plane, the associated first-passage and first-hitting time PDFs to locate these disks would move this problem closer to biological reality. One might think of, as an example, a bee searching for flowers, a situation amenable to experiments [110]. Measuring the first-passage and first-hitting time PDFs may help to put the LF foraging hypothesis on more rigorous theoretical grounds, which is a long-standing open problem.

Another interesting direction to study is the combination of Lévy-type processes with resetting, as studied, for instance, for mean first passage and arrival times in [111]. Moreover, it will be interesting to explore in more detail the impact of a bias on the first-passage and first-hitting time PDFs similar to the analyses in [80, 81]. Biologically this would relate to the problem of chemotaxis when cells migrate according to a chemical concentration gradient to find inflammation sites [112]. Similarly, extensions of the present results in general external potential fields [113] should be studied, including phenomena such as barrier crossing, stochastic resonant activation, and noise-enhanced stability phenomena [114]. Further applications to pursue include population dynamics and biophysical models [115], as well as the modelling of the dynamics in Josephson junctions [116], to mention but a few stray examples. We moreover note that it should be analysed how distributed transport parameters (such as K_α) may modify the results for first-passage and first-hitting, similar to what happens for Brownian processes [117]. Finally, it will be interesting to study more complex, many-body scenarios such as hunting in flocks [118].

Acknowledgments

VVP acknowledges fruitful discussions with Olivier Bénichou. RM and AVC acknowledge financial support from Deutsche Forschungsgemeinschaft (Grant numbers ME 1535/6-1 and ME 1535/7-1). RM also acknowledges an Alexander von Humboldt Honorary Research Scholarship from the Foundation for Polish Science. NW and GB were funded at Potsdam and Dresden, respectively, by ONR Global NICOP grant N62909-15-1-N143 to the CFSA, University of Warwick, and they wish to thank the PI, Sandra Chapman. RK thanks Sabine Klapp and Holger Stark, TU Berlin, for their hospitality as a guest scientist as well as ONR Global for financial support. He also acknowledges funding from the London Mathematical Laboratory, where he is an External Fellow. We acknowledge the support of Deutsche Forschungsgemeinschaft (German Research Foundation) and Open Access Publication Fund of Potsdam University.

Appendix A. Short-time behaviour of the first-passage of Lévy flights

The finite value p_{jump} of the jump in the short-time behaviour of LFs (figure 4) can be estimated by computing the survival probability at short times by using the asymptotic expression for large x . For the purpose of this derivation we assume that the starting position is at $x = 0$ while the boundary is at $x = x_0$, which is physically identical to our original setting. The survival probability at short times reads

$$\mathcal{S}(t) = \int_{-\infty}^{x_0} f_\alpha(t, x) dx, \quad (\text{A.1})$$

where the symmetric Lévy stable PDF in the limit $|x| \rightarrow \infty$ is [37, 56]

$$f_\alpha(t, x) \sim C_1(\alpha) \frac{K_\alpha t}{|x|^{1+\alpha}}, \quad C_1(\alpha) = \frac{1}{\pi} \sin(\pi\alpha/2) \Gamma(1 + \alpha). \quad (\text{A.2})$$

The first-passage time density is the negative derivative of the survival probability,

$$\wp_{\text{PF}}(t) = -\frac{d\mathcal{S}(t)}{dt}. \quad (\text{A.3})$$

Conversely,

$$1 - \mathcal{S}(t) = \int_{x_0}^{\infty} f_\alpha(t, x) dx = \frac{C_1(\alpha) K_\alpha t}{\alpha x_0^\alpha}. \quad (\text{A.4})$$

Hence

$$p_{\text{jump}} = \wp_{\text{PF}}(t \rightarrow 0) = \frac{K_\alpha \sin(\pi\alpha/2)\Gamma(\alpha)}{\pi x_0^\alpha}. \quad (\text{A.5})$$

In order to estimate the slope at $t = 0$ we will compute whether the values of the PDF increase or decrease at short times. As we established above the probability to cross a boundary within an infinitesimal time Δt_1 reads

$$p_1 = 1 - \mathcal{S}(\Delta t_1) = \int_{x_0}^{\infty} f_\alpha(\Delta t_1, x) dx = \frac{C_1(\alpha)K_\alpha \Delta t_1}{\alpha x_0^\alpha}. \quad (\text{A.6})$$

The probability to be in the vicinity of some $x \leq x_0$ after Δt_1 is $f_\alpha(\Delta t_1, x) dx$. Concurrently the probability to cross the boundary in time Δt_2 after the original time interval Δt_1 if a walker landed at x is $\int_{x_0-x}^{\infty} f_\alpha(\Delta t_2, x) dx$. Hence the probability to cross the boundary within $(\Delta t_1, \Delta t_2 + \Delta t_1)$ becomes

$$p_2 = \int_{-\infty}^{x_0} dx_1 \int_{x_0-x_1}^{\infty} f_\alpha(\Delta t_1, x_1) f_\alpha(\Delta t_2, x_2) dx_2. \quad (\text{A.7})$$

For simplicity we assume that $\Delta t_1 = \Delta t_2$. Then,

$$\begin{aligned} p_2 &= \int_{-\infty}^{\infty} dx_1 \int_{x_0-x_1}^{\infty} f_\alpha(\Delta t_1, x_1) f_\alpha(\Delta t_1, x_2) dx_2 \\ &\quad - \int_{x_0}^{\infty} dx_1 \int_{x_0-x_1}^{\infty} f_\alpha(\Delta t_1, x_1) f_\alpha(\Delta t_1, x_2) dx_2 \\ &= \int_{-\infty}^{\infty} dx_1 \int_{x_0}^{\infty} f_\alpha(\Delta t_1, x_1) f_\alpha(\Delta t_1, x_2) dx_2 \\ &\quad + \int_{-\infty}^{\infty} dx_1 \int_{x_0-x_1}^{x_0} f_\alpha(\Delta t_1, x_1) f_\alpha(\Delta t_1, x_2) dx_2 \\ &\quad - \int_{x_0}^{\infty} dx_1 \int_{x_0}^{\infty} f_\alpha(\Delta t_1, x_1) f_\alpha(\Delta t_1, x_2) dx_2 \\ &\quad - \int_{x_0}^{\infty} dx_1 \int_{x_0-x_1}^{x_0} f_\alpha(\Delta t_1, x_1) f_\alpha(\Delta t_1, x_2) dx_2 \\ &= p_1 - p_1^2 + \int_{-\infty}^{x_0} dx_1 \int_{x_0-x_1}^{x_0} f_\alpha(\Delta t_1, x_1) f_\alpha(\Delta t_1, x_2) dx_2. \end{aligned} \quad (\text{A.8})$$

The latter integral can be computed analytically as follows,

$$\begin{aligned} &\int_{-\infty}^{x_0} dx_1 \int_{x_0-x_1}^{x_0} f_\alpha(\Delta t_1, x_1) f_\alpha(\Delta t_1, x_2) dx_2 \\ &= (C_1(\alpha)K_\alpha \Delta t_1)^2 \int_{-\infty}^{x_0} \frac{dx_1}{|x_1|^{1+\alpha}} \int_{x_0-x_1}^{x_0} \frac{dx_2}{|x_2|^{1+\alpha}} \\ &= \frac{(C_1(\alpha)K_\alpha \Delta t_1)^2}{x_0^{2\alpha}} \int_{-\infty}^1 \frac{dx_1'}{|x_1'|^{1+\alpha}} \int_{1-x_1'}^1 \frac{dx_2'}{x_2'^{1+\alpha}} \\ &= \frac{(C_1(\alpha)K_\alpha \Delta t_1)^2}{\alpha x_0^{2\alpha}} \int_{-\infty}^1 \frac{dx_1'}{|x_1'|^{1+\alpha}} \left(\frac{1}{(1-x_1')^\alpha} - 1 \right). \end{aligned} \quad (\text{A.9})$$

In order to get an analytical result for the last integral we will split it into two parts from $-\infty$ to 0 and from 0 to 1. The first part without the prefactor is

$$\begin{aligned} &\int_{-\infty}^0 \frac{dx_1'}{|x_1'|^{1+\alpha}} \left(\frac{1}{(1-x_1')^\alpha} - 1 \right) \\ &= \int_0^{\infty} \frac{dy}{y^{1+\alpha}} \left(\frac{1-(1+y)^\alpha}{(1+y)^\alpha} \right) \\ &= \int_0^{\infty} z^{\alpha-1} \left(\frac{1}{(1+1/z)^\alpha} - 1 \right) dz \\ &= \int_0^{\infty} z^{2\alpha-1} ((z+1)^{-\alpha} - z^{-\alpha}) dz = B(2\alpha, -\alpha), \end{aligned} \quad (\text{A.10})$$

where $B(x, y)$ stands for the beta function and the last equality follows from formula 2.2.12.5 in [119] and is valid for $0 < \alpha < 1$. The second part produces

$$\begin{aligned}
& \int_0^1 \frac{dx'_1}{x'^{1+\alpha}_1} \left(\frac{1}{(1-x'_1)^\alpha} - 1 \right) \\
&= \int_0^1 \frac{dy}{(1-y)^{1+\alpha}} \left(\frac{1}{y^\alpha} - 1 \right) \\
&= \lim_{z \rightarrow 1} \int_0^1 \frac{dy}{(1-zy)^{1+\alpha}} \left(\frac{1}{y^\alpha} - 1 \right) \\
&= \lim_{z \rightarrow 1} \left\{ \int_0^1 y^{-\alpha+1-1} (1-y)^{2-\alpha-(1-\alpha)-1} (1-zy)^{-1-\alpha} dy - \frac{1}{\alpha z} (1-zu)^{-\alpha} \Big|_{u=0}^1 \right\} \\
&= \lim_{z \rightarrow 1} \left\{ \frac{\Gamma(1-\alpha)}{\Gamma(2-\alpha)} {}_2F_1(1+\alpha, 1-\alpha, 2-\alpha; z) - \frac{1}{\alpha z} \frac{1}{(1-z)^\alpha} + \frac{1}{\alpha z} \right\}, \tag{A.11}
\end{aligned}$$

where ${}_2F_1(1+\alpha, 1-\alpha, 2-\alpha; z)$ is the hypergeometric function obtained through the integral definition which is valid in this case for $\alpha < 1$. This hypergeometric function can be transformed according to 15.3.6 from [120] as follows

$$\begin{aligned}
{}_2F_1(1+\alpha, 1-\alpha, 2-\alpha; z) &= \frac{\Gamma(2-\alpha)\Gamma(-\alpha)}{\Gamma(1-2\alpha)} {}_2F_1(1+\alpha, 1-\alpha, 1+\alpha; 1-z) \\
&\quad + (1-z)^{-\alpha} \frac{\Gamma(2-\alpha)\Gamma(\alpha)}{\Gamma(1+\alpha)\Gamma(1-\alpha)} {}_2F_1(1-2\alpha, 1, 1-\alpha; 1-z). \tag{A.12}
\end{aligned}$$

For $z \rightarrow 1$ the hypergeometric functions in the last expression will converge to 1. Assembling all of the pieces we obtain the following formula,

$$\int_0^1 \frac{dx}{x^{1+\alpha}} \left(\frac{1}{(1-x)^\alpha} - 1 \right) = \frac{1}{\alpha} + \frac{\Gamma(1-\alpha)\Gamma(-\alpha)}{\Gamma(1-2\alpha)} = \frac{1}{\alpha} - \frac{4^\alpha \sqrt{\pi} \Gamma(1-\alpha)}{\alpha \Gamma(1/2-\alpha)}. \tag{A.13}$$

Finally, collecting all the contributions to p_2 we get

$$\begin{aligned}
p_2 &= p_1 - p_1^2 + p_1^2 \left(1 - \frac{4^\alpha \sqrt{\pi} \Gamma(1-\alpha)}{\Gamma(1/2-\alpha)} - \frac{\Gamma(1-\alpha)\Gamma(2\alpha)}{\Gamma(\alpha)} \right) \\
&= p_1 + p_1^2 \left(\frac{4^\alpha \sqrt{\pi} \alpha \Gamma(-\alpha)}{\Gamma(1/2-\alpha)} - \frac{\Gamma(1-\alpha)\Gamma(2\alpha)}{\Gamma(\alpha)} \right) \\
&= p_1 - p_1^2 \frac{4^\alpha \pi^{3/2} (1+2\cos(\pi\alpha))}{\Gamma(1/2-\alpha)\Gamma(\alpha)\sin(2\pi\alpha)}. \tag{A.14}
\end{aligned}$$

The last expression clearly shows that with decreasing α at $\alpha = 2/3$ the probability to cross the boundary within an interval of time $(\Delta t_1, 2\Delta t_1)$ gets lower than p_1 due to the change in sign of the second term in (A.14). Thus, $\wp_{\text{PF}}(t)$ decreases for $\alpha < 2/3$ at short t and at first grows for $\alpha > 2/3$.

Appendix B. Derivation of the average time of jump, the jump duration distribution and its long-time expansion for Lévy walks, $1 < \alpha \leq 2$

In order to estimate the effective diffusion coefficient of LWs one has to know the distribution of durations of the jumps, the average jump duration as well as its long-time behaviour. The characteristic function of a symmetric Lévy stable process is

$$\phi(k) = \exp(-\sigma_0^\alpha |k|^\alpha). \tag{B.1}$$

The distribution of the jump lengths can be expressed in terms of Fox H -functions as [15, 121]

$$f_\alpha(x) = \int_0^\infty \frac{dk}{\pi} \cos(kx) e^{-\sigma_0^\alpha |k|^\alpha} = \frac{1}{\sqrt{\pi} x} H_{12}^{11} \left[\frac{x^\alpha}{2^\alpha \sigma_0^\alpha} \left| \begin{matrix} (1, 1) \\ (\frac{1}{2}, \frac{\alpha}{2}), (1, \frac{\alpha}{2}) \end{matrix} \right. \right].$$

The jump duration is coupled to the jump length distribution, $\tau(x) = \left\lfloor \frac{x}{v_0} \right\rfloor$. Then the relocation time distribution reads

$$\begin{aligned}
\psi(\tau) &= \int_{-\infty}^\infty dx \delta(\tau - \tau(x)) f_\alpha(x) = \int_{-\infty}^\infty dx \delta\left(\tau - \left\lfloor \frac{x}{v_0} \right\rfloor\right) f_\alpha(x) \\
&= \int_{-\infty}^0 dx \delta\left(\tau + \frac{x}{v_0}\right) f_\alpha(x) + \int_0^\infty dx \delta\left(\tau - \frac{x}{v_0}\right) f_\alpha(x) \\
&= 2 \int_0^\infty dx \delta\left(\frac{x}{v_0} - \tau\right) f_\alpha(x) = 2v_0 f_\alpha(v_0 \tau). \tag{B.2}
\end{aligned}$$

Hence, $\psi(\tau)$ yields in the form

$$\psi(\tau) = \frac{2}{\sqrt{\pi}\tau} H_{12}^{11} \left[\frac{v_0^\alpha}{2^\alpha \sigma_0^\alpha} \tau^\alpha \left| \begin{matrix} (1, 1) \\ (\frac{1}{2}, \frac{\alpha}{2}), (1, \frac{\alpha}{2}) \end{matrix} \right. \right]. \quad (\text{B.3})$$

One can easily check that the latter function is properly normalised, $\int_0^\infty \psi(\tau) d\tau = 1$. The average jump duration can be computed for $\alpha > 1$ (otherwise it diverges) as

$$\begin{aligned} \langle \tau \rangle &= \int_0^\infty d\tau \tau \psi(\tau) = \frac{2}{\sqrt{\pi}} \int_0^\infty d\tau H_{12}^{11} \left[\frac{v_0^\alpha}{2^\alpha \sigma_0^\alpha} \tau^\alpha \left| \begin{matrix} (1, 1) \\ (\frac{1}{2}, \frac{\alpha}{2}), (1, \frac{\alpha}{2}) \end{matrix} \right. \right] \\ &= \frac{2}{\alpha \sqrt{\pi}} \int_0^\infty dt t^{1/\alpha-1} H_{12}^{11} \left[\frac{v_0^\alpha}{2^\alpha \sigma_0^\alpha} t \left| \begin{matrix} (1, 1) \\ (\frac{1}{2}, \frac{\alpha}{2}), (1, \frac{\alpha}{2}) \end{matrix} \right. \right] \\ &= \frac{2}{\alpha \sqrt{\pi}} \left(\frac{2\sigma}{v_0} \right)^{\frac{1}{\alpha}} \Gamma \left[\frac{\frac{1}{2} + \frac{\alpha/2}{\alpha}, 1 - 1 - 1/\alpha}{1 - 1 - \frac{\alpha/2}{\alpha}} \right] \\ &= \frac{4}{\alpha \sqrt{\pi}} \frac{\sigma_0}{v_0} \frac{\Gamma(-\frac{1}{\alpha})}{\Gamma(-\frac{1}{2})} = \frac{2\sigma_0}{\pi v_0} \Gamma \left(1 - \frac{1}{\alpha} \right), \end{aligned} \quad (\text{B.4})$$

using the properties of the H -function [121]. Our result exactly coincides with equation (54) in [57], where it was derived as an approximate formula. We show here that it is actually an exact expression (the factor v_0 missing in the corresponding equation of [57] is just a misprint there). From the distribution we obtain the exact form in Laplace space and expand it at small s corresponding to long times. The Laplace transform of equation (B.2) reads [121]

$$\begin{aligned} \mathcal{L}(\psi(\tau)) &= \tilde{\psi}(s) = \mathcal{L} \left(\frac{2}{\sqrt{\pi}\tau} H_{12}^{11} \left[\frac{v_0^\alpha}{2^\alpha \sigma_0^\alpha} \tau^\alpha \left| \begin{matrix} (1, 1) \\ (\frac{1}{2}, \frac{\alpha}{2}), (1, \frac{\alpha}{2}) \end{matrix} \right. \right] \right) \\ &= \frac{2}{\sqrt{\pi}} H_{22}^{12} \left[\frac{v_0^\alpha}{2^\alpha \sigma_0^\alpha} s^{-\alpha} \left| \begin{matrix} (1, \alpha), (1, 1) \\ (\frac{1}{2}, \frac{\alpha}{2}), (1, \frac{\alpha}{2}) \end{matrix} \right. \right] \\ &= \frac{2}{\sqrt{\pi}} H_{22}^{21} \left[\frac{2^\alpha \sigma_0^\alpha}{v_0^\alpha} s^\alpha \left| \begin{matrix} (\frac{1}{2}, \frac{\alpha}{2}), (0, \frac{\alpha}{2}) \\ (0, \alpha), (0, 1) \end{matrix} \right. \right]. \end{aligned} \quad (\text{B.5})$$

The expansion of the latter H -function for $s \rightarrow 0$ has a ratio of nominally infinite values due to the presence of zeros among the coefficients. In order to solve this problem we introduce the infinitesimal parameter ε and treat the H -function as a limit of another H -function with non-zero coefficients ε , namely,

$$H_{22}^{21} \left[\frac{2^\alpha \sigma_0^\alpha}{v_0^\alpha} s^\alpha \left| \begin{matrix} (\frac{1}{2}, \frac{\alpha}{2}), (0, \frac{\alpha}{2}) \\ (0, \alpha), (0, 1) \end{matrix} \right. \right] = \lim_{\varepsilon \rightarrow 0} H_{22}^{21} \left[\frac{2^\alpha \sigma_0^\alpha}{v_0^\alpha} s^\alpha \left| \begin{matrix} (\frac{1}{2}, \frac{\alpha}{2}), (\varepsilon, \frac{\alpha}{2}) \\ (\varepsilon, \alpha), (\varepsilon, 1) \end{matrix} \right. \right]. \quad (\text{B.6})$$

The expansion of the latter H -function reads ([119, 121]),

$$\begin{aligned} H_{22}^{21} \left[z \left| \begin{matrix} (\frac{1}{2}, \frac{\alpha}{2}), (\varepsilon, \frac{\alpha}{2}) \\ (\varepsilon, \alpha), (\varepsilon, 1) \end{matrix} \right. \right] &= \sum_{k=0}^{\infty} \frac{2\Gamma(\varepsilon - \frac{1}{\alpha}(\varepsilon + k)) \Gamma(\frac{1}{2} + \frac{1}{2}(\varepsilon + k))}{\sqrt{\pi}\Gamma(\varepsilon - \frac{1}{2}(\varepsilon + k))} \frac{(-1)^k z^{(\varepsilon+k)/\alpha}}{k! \alpha} \\ &\quad + \sum_{k=0}^{\infty} \frac{2\Gamma(\varepsilon - \alpha(\varepsilon + k)) \Gamma(\frac{1}{2} + \frac{1}{2}(\varepsilon + k))}{\sqrt{\pi}\Gamma(\varepsilon - \frac{1}{2}(\varepsilon + k))} \frac{(-1)^k z^{\varepsilon+k}}{k!}, \end{aligned} \quad (\text{B.7})$$

where $z = 2^\alpha \sigma_0^\alpha s^\alpha / (v_0^\alpha)$. Using the known behaviour of the Gamma function for small arguments, $\Gamma(\varepsilon) \sim 1/\varepsilon$, we obtain the following expansion,

$$\psi(s) \sim 1 - \langle \tau \rangle s + A s^\alpha + \dots, \quad (\text{B.8})$$

where 1 has contributions from zeroth orders of both sums, $\langle \tau \rangle$ is given by expression (B.4), and A reads

$$A = -\frac{2^{\alpha+1} \sigma_0^\alpha}{\sqrt{\pi} v_0^\alpha} \frac{\Gamma(-\alpha) \Gamma(1/2 + \alpha/2)}{\Gamma(-\alpha/2)} = \frac{\sigma_0^\alpha}{v_0^\alpha |\cos(\pi\alpha/2)|}. \quad (\text{B.9})$$

This form can be shown to be equivalent to the corresponding expression in [57].

Appendix C. Derivation of the effective long-time diffusion coefficient of LWs, $1 < \alpha \leq 2$

Let us start from equation (29) in [20],

$$P(k, s) = \frac{[\tilde{\Psi}(s + ik\nu) + \tilde{\Psi}(s - ik\nu)]P_0(k)}{2 - [\psi(s + ik\nu) + \psi(s - ik\nu)]}, \quad (\text{C.1})$$

where $\tilde{\Psi}(s)$ is the Laplace transform of the survival probability and can be expressed through $\psi(s)$ as $\tilde{\Psi}(s) = [1 - \psi(s)]/s$, and for long times (small s) we have $\psi(s) \sim 1 - \langle\tau\rangle s + As^\alpha$. Hence,

$$P(k, s) \sim \frac{P_0(k)[2\langle\tau\rangle - A((s + ik\nu)^{\alpha-1} + (s - ik\nu)^{\alpha-1})]}{2s\langle\tau\rangle - A((s + ik\nu)^\alpha + (s - ik\nu)^\alpha)}. \quad (\text{C.2})$$

The expressions in the round brackets can be expanded,

$$(s \pm ik\nu)^\alpha \sim e^{\pm \frac{i\pi\alpha}{2}} |k|^\alpha \nu_0^\alpha \left(1 \pm \frac{s\alpha}{ik\nu}\right). \quad (\text{C.3})$$

The last expansion assumes the condition $s \ll |k|\nu_0 \ll 1$. After neglecting higher powers in s one gets

$$P(k, s) = \frac{P_0(k)}{s - A|k|^\alpha \nu_0^\alpha \cos\left(\frac{\pi\alpha}{2}\right) / \langle\tau\rangle}. \quad (\text{C.4})$$

Alternatively,

$$P(k, s) = \frac{P_0(k)}{s + K_\alpha^{\text{LW}} |k|^\alpha}, \quad (\text{C.5})$$

where

$$\begin{aligned} K_\alpha^{\text{LW}} &= \frac{A\nu_0^\alpha \left| \cos\left(\frac{\pi\alpha}{2}\right) \right|}{\langle\tau\rangle} = \frac{2\sigma_0^\alpha \sin\left(\frac{\pi\alpha}{2}\right) \Gamma(-\alpha) \Gamma(1+\alpha) \left| \cos\left(\frac{\pi\alpha}{2}\right) \right|}{\pi \langle\tau\rangle} \\ &= \frac{\sigma_0^{\alpha-1} \sin\left(\frac{\pi\alpha}{2}\right) \Gamma(-\alpha) \Gamma(1+\alpha) \left| \cos\left(\frac{\pi\alpha}{2}\right) \right| \nu_0}{\Gamma\left(1 - \frac{1}{\alpha}\right)} \\ &= \frac{\sigma_0^\alpha}{\langle\tau\rangle}, \end{aligned} \quad (\text{C.6})$$

where $\langle\tau\rangle$ is given by equation (B.4). The last result is exactly the intuitive definition of the diffusivity from a continuous time random walk perspective. The second line in equation (C.6) corrects the formula (55) in [57].

Appendix D. Estimation of the jump in the first-passage time PDF of LWs

The jump in the first-passage time PDF of LWs corresponds to the probability stored in the ballistically moving front peak of the position PDF [20]. The density of particles in these peaks reads (equation (32) in [20])

$$G_{\text{front}}(x, t) = \frac{1}{2} \Psi(t) (\delta(x - \nu t) + \delta(x + \nu t)). \quad (\text{D.1})$$

From the equations above we can compute the survival probability as a function of time. In Laplace space $\tilde{\Psi}(s) = [1 - \psi(s)]/s$. From expression (B.5),

$$\frac{\tilde{\psi}(s)}{s} = \frac{2}{\sqrt{\pi}s} H_{22}^{21} \left[\frac{2^\alpha \sigma_0^\alpha}{\nu_0^\alpha} s^\alpha \left| \begin{matrix} \left(\frac{1}{2}, \frac{\alpha}{2}\right), \left(0, \frac{\alpha}{2}\right) \\ (0, \alpha), (0, 1) \end{matrix} \right. \right]. \quad (\text{D.2})$$

Its inverse Laplace transform reads [121],

$$\begin{aligned} \mathcal{L}^{-1}\left(\frac{\tilde{\psi}(s)}{s}\right) &= \frac{2}{\sqrt{\pi}} H_{32}^{21} \left[\frac{2^\alpha \sigma_0^\alpha}{\nu_0^\alpha} t^{-\alpha} \left| \begin{matrix} \left(\frac{1}{2}, \frac{\alpha}{2}\right), \left(0, \frac{\alpha}{2}\right), (1, \alpha) \\ (0, \alpha), (0, 1) \end{matrix} \right. \right] \\ &= \frac{2}{\sqrt{\pi}} H_{23}^{12} \left[\frac{\nu_0^\alpha}{2^\alpha \sigma_0^\alpha} t^\alpha \left| \begin{matrix} (1, \alpha), (1, 1) \\ \left(\frac{1}{2}, \frac{\alpha}{2}\right), \left(1, \frac{\alpha}{2}\right), (0, \alpha) \end{matrix} \right. \right]. \end{aligned} \quad (\text{D.3})$$

The survival probability as a function of t is then

$$\Psi(t) = 1 - \frac{2}{\sqrt{\pi}} H_{23}^{12} \left[\frac{v_0^\alpha}{2^\alpha \sigma_0^\alpha} t^\alpha \left| \begin{matrix} (1, \alpha), (1, 1) \\ \left(\frac{1}{2}, \frac{\alpha}{2}\right), \left(1, \frac{\alpha}{2}\right), (0, \alpha) \end{matrix} \right. \right]. \quad (\text{D.4})$$

This is an exact analytical result. The value of this H -function can be found from an expansion in t [119],

$$\begin{aligned} & H_{23}^{12} \left[\frac{v_0^\alpha}{2^\alpha \sigma_0^\alpha} t^\alpha \left| \begin{matrix} (1, \alpha), (1, 1) \\ \left(\frac{1}{2}, \frac{\alpha}{2}\right), \left(1, \frac{\alpha}{2}\right), (0, \alpha) \end{matrix} \right. \right] \\ &= \frac{2}{\alpha} \sum_{k=0}^{\infty} \frac{\Gamma(2k+1) \Gamma\left(\frac{2k+1}{\alpha}\right)}{\Gamma\left(k+\frac{1}{2}\right) \Gamma(2+2k)} \left(\frac{v_0 t}{2\sigma_0}\right)^{1+2k} \frac{(-1)^k}{k!}. \end{aligned} \quad (\text{D.5})$$

The last two equations allow one to compute the value of G_{front} . Unless the argument of the H -function is too big the series (D.5) converges quite fast.

Appendix E. Derivation of the long-time limit of the first-hitting time PDF of LFs, $1 < \alpha \leq 2$

We start from equation (9). The integral in the numerator can be computed analytically and reads

$$\int_{-\infty}^{\infty} dk \frac{1}{s + K_\alpha |k|^\alpha} = \frac{2\pi}{\alpha \sin(\pi/\alpha)} \frac{s^{1/\alpha-1}}{K_\alpha^{1/\alpha}}. \quad (\text{E.1})$$

Hence equation (9) can be rewritten as

$$\wp_{\text{HF}}(s) = \frac{\alpha \sin(\pi/\alpha) K_\alpha^{1/\alpha}}{\pi} \int_0^\infty dk \frac{s^{1-1/\alpha}}{s + K_\alpha |k|^\alpha} \cos(kx_0). \quad (\text{E.2})$$

From the relation (1.80) in [122] we know that

$$t^{\beta-1} E_{\alpha,\beta}(-at^\alpha) \div \frac{s^{\alpha-\beta}}{s^\alpha + a}, \quad (\text{E.3})$$

where \div stands as a notation for the Laplace transform pair and $E_{\alpha,\beta}(t)$ is the two-parameter Mittag-Leffler function. Hence, we get equation (10),

$$\wp_{\text{HF}}(t) = \frac{\alpha \sin(\pi/\alpha) K_\alpha^{1/\alpha}}{\pi} t^{1/\alpha-1} \int_0^\infty dk \cos(kx_0) E_{1,1/\alpha}(-K_\alpha k^\alpha t). \quad (\text{E.4})$$

This equation clearly shows that for $\alpha = 1$ the PDF of first-hitting the target is exactly zero, $\wp_{\text{HF}} = 0$ (the prefactor is equal to zero in this case). Now we consider the long-time limit $t \rightarrow \infty$. Rewriting the previous equation as

$$\begin{aligned} \wp_{\text{HF}}(t) &= \frac{\alpha \sin(\pi/\alpha) K_\alpha^{1/\alpha}}{\pi} t^{1/\alpha-1} \int_0^\infty dk E_{1,1/\alpha}(-K_\alpha k^\alpha t) \\ &\quad - \frac{\alpha \sin(\pi/\alpha) K_\alpha^{1/\alpha}}{\pi} t^{1/\alpha-1} \int_0^\infty dk (1 - \cos(kx_0)) E_{1,1/\alpha}(-K_\alpha k^\alpha t). \end{aligned} \quad (\text{E.5})$$

Consider separately the first and the second contribution. The first integral is zero,

$$\begin{aligned} \int_0^\infty dk E_{1,1/\alpha}(-K_\alpha k^\alpha t) &\sim (K_\alpha t)^{-1/\alpha} \int_0^\infty dk' E_{1,1/\alpha}(-k'^\alpha) \\ &\sim \frac{1}{\alpha} (K_\alpha t)^{-1/\alpha} \int_0^\infty y^{1/\alpha-1} E_{1,1/\alpha}(-y) dy \\ &\sim \lim_{z \rightarrow \infty} \int_0^z y^{1/\alpha-1} E_{1,1/\alpha}(-y) dy \\ &\sim \lim_{z \rightarrow \infty} z^{1/\alpha} E_{1,1+1/\alpha}(-z) \\ &\sim \lim_{z \rightarrow \infty} z^{1/\alpha} \frac{1}{z} = 0, \end{aligned} \quad (\text{E.6})$$

where we used formula (1.99) in [122]. In the second integral the Mittag-Leffler function can be substituted by its large argument limit, $E_{1,1/\alpha}(-K_\alpha k^\alpha t) \rightarrow -1/[K_\alpha k^\alpha t \Gamma(1/\alpha - 1)]$, because at small values of k the expression $(1 - \cos(kx_0))$ disappears. Then,

$$\begin{aligned}
\wp_{\text{HF}}(t) &= -\frac{\alpha \sin\left(\frac{\pi}{\alpha}\right) K_{\alpha}^{1/\alpha-1}}{\pi \Gamma(1/\alpha-1) t^{1/\alpha-2}} \int_0^{\infty} \frac{1 - \cos(kx_0)}{k^{\alpha}} dk \\
&= -\frac{\alpha \sin\left(\frac{\pi}{\alpha}\right)}{\pi \Gamma(1/\alpha-1)} \frac{\Gamma(2-\alpha) \sin\left(\frac{\pi\alpha}{2}\right)}{\alpha-1} x_0^{\alpha-1} K_{\alpha}^{1/\alpha-1} t^{1/\alpha-2} \\
&= \frac{\sin\left(\frac{\pi}{\alpha}\right) \Gamma(2-\alpha) \sin\left(\frac{\pi\alpha}{2}\right)}{\pi \Gamma(1/\alpha)} x_0^{\alpha-1} K_{\alpha}^{1/\alpha-1} t^{1/\alpha-2},
\end{aligned} \tag{E.7}$$

which exactly coincides with result (A.9) in [61] and is equivalent to the corresponding expression in [98].

Appendix F. Derivation of the short-time limit of the first-hitting time PDF of LFs

Here we compute the power-law of the first-hitting time PDF of LFs in the limit of short times. It is again convenient to start from equation (10). We change the variable as $y = k(K_{\alpha}t)^{1/\alpha}$. Hence,

$$\wp_{\text{HF}}(t) = \frac{\alpha \sin(\pi/\alpha)}{\pi} t^{-1} \int_0^{\infty} dy \cos\left(\frac{yx_0}{(K_{\alpha}t)^{1/\alpha}}\right) E_{1,1/\alpha}(-y^{\alpha}). \tag{F.1}$$

Introducing the notation $\lambda = x_0/(K_{\alpha}t)^{1/\alpha}$ and using the definition of the Mittag-Leffler function,

$$\begin{aligned}
\wp_{\text{HF}}(t) &= \frac{\alpha \sin(\pi/\alpha)}{\pi} t^{-1} \int_0^{\infty} dy \cos(\lambda y) \sum_{n=0}^{\infty} \frac{(-y^{\alpha})^n}{\Gamma(n+1/\alpha)} \\
&= \frac{\alpha \sin(\pi/\alpha)}{\pi} t^{-1} \sum_{n=0}^{\infty} \int_0^{\infty} dy \cos(\lambda y) \frac{(-y^{\alpha})^n}{\Gamma(n+1/\alpha)} = \sum_{n=0}^{\infty} I_n(t),
\end{aligned} \tag{F.2}$$

where $I_n(t)$ is the n th term of the expansion of $\wp_{\text{HF}}(t)$ in a power series. With the help of equation (2.25) for improper integrals in [123],

$$\int_0^{\infty} \tau^k e^{-i\omega\tau} d\tau = \frac{\Gamma(k+1)}{\omega^{k+1}} e^{-\frac{1}{2}(k+1)\pi i} \tag{F.3}$$

we compute the terms one by one. For convenience we use the shorthand notation $C(\alpha) = \frac{\alpha \sin(\pi/\alpha)}{\pi}$. Then,

$$\begin{aligned}
I_0(t) &= C(\alpha) t^{-1} \frac{1}{\Gamma(1/\alpha)} \int_0^{\infty} dy \cos(\lambda y) = 0, \\
I_1(t) &= C(\alpha) t^{-1} \frac{-1}{\Gamma(1+1/\alpha)} \frac{\Gamma(\alpha+1)}{\lambda^{\alpha+1}} \text{Re}[(-i)^{\alpha+1}] \\
&= C(\alpha) t^{-1} \frac{-1}{\Gamma(1+1/\alpha)} \frac{\Gamma(\alpha+1)}{\lambda^{\alpha+1}} \text{Re}\left[\exp\left(-\frac{i\pi}{2}(1+\alpha)\right)\right] \\
&= -C(\alpha) t^{-1} \frac{-1}{\Gamma(1+1/\alpha)} \frac{\Gamma(\alpha+1)}{\lambda^{\alpha+1}} \sin\left(\frac{\pi\alpha}{2}\right) \\
&= C(\alpha) \frac{\Gamma(1+\alpha) \sin(\pi\alpha/2)}{\Gamma(1+1/\alpha)} \frac{K_{\alpha}^{1+1/\alpha}}{x_0^{\alpha+1}} t^{1/\alpha},
\end{aligned} \tag{F.4}$$

$$I_2(t) = C(\alpha) \frac{\Gamma(2\alpha+1)}{\Gamma(2+1/\alpha)(-\sin(\pi\alpha))} \frac{K_{\alpha}^{2+1/\alpha}}{x_0^{2\alpha+1}} t^{1+1/\alpha}, \tag{F.5}$$

$$I_3(t) = C(\alpha) \frac{\Gamma(3\alpha+1)}{\Gamma(3+1/\alpha)(-\sin(3\pi\alpha/2))} \frac{K_{\alpha}^{3+1/\alpha}}{x_0^{3\alpha+1}} t^{2+1/\alpha}. \tag{F.6}$$

Appendix G. The target size selection in the simulations

Our theoretical framework for LFs includes the notion of a point-like target. However, in the simulations the target size should be non-zero if the target is to be successfully located. Thus the target should not be too small such that it can actually be hit successfully. At the same time it should not be too large, otherwise this would result in the scenario of the first-passage, and thus the scaling exponent would converge to the universal Sparre-Andersen result. One has to choose the target size correctly. From the theory the asymptotic behaviour at long times is known to be $\wp_{\text{HF}}(t) \simeq t^{1/\alpha-2}$ [98]. In figure G1 we show how the exponent at long times depends on the target size for the time resolution $\delta t = 0.001$. For very small targets the exponent is closer to -1 (data 1 in figure G1) and the Sparre-Andersen limit can be obtained when large targets are considered (data set 4 in figure G1 corresponds to the case in which the starting point was distance 1 away from the boundary of the target with $d = 10$). We also checked that this automatically leads to the proper power law with scaling exponent $1/\alpha$ at short times. Vice versa one could use the short-time power law to get the best fit target size with the correct long-term first-hitting PDF statistics. Note that in order to get the exponents in figure G1 we averaged the data in the time interval [50, 1000]. For any fixed d and δt the exponent decreases slightly when the frame of averaging is

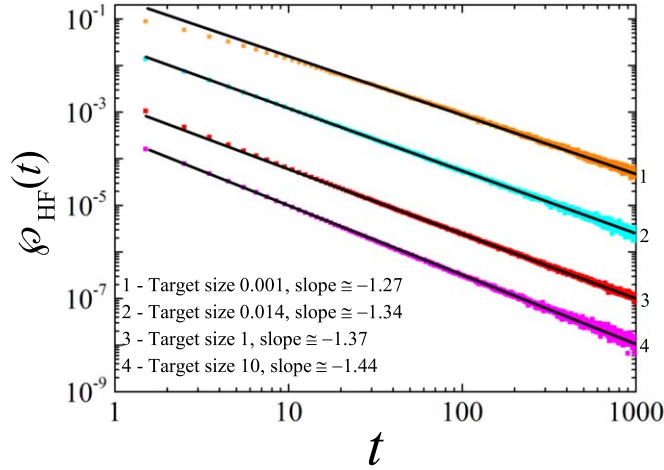


Figure G1. Dependence of the long-time exponent of the PDF of first-hitting on the target size for LFs. Note that for better visual comparison of the PDFs their values were divided by a factor of 10 for $d = 0.014$, of 100 for $d = 1$, and of 1000 for $d = \infty$. In the first three cases the target was centred at $x = 0$. For $d = 10$ the target is centred at $x = -5$. Parameters: $\alpha = 1.5$, $K_\alpha = 1$, $x_0 = 1$, and $\delta t = 0.001$. The number of runs is 2×10^6 .

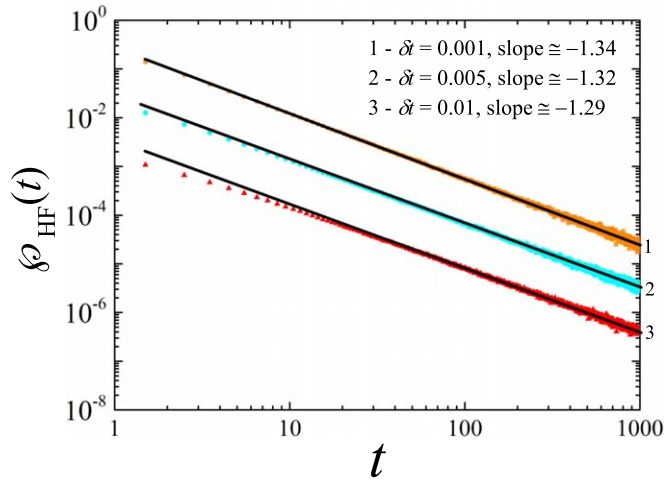


Figure G2. Dependence of the long-time exponent of the PDF of first-hitting on the time resolution in the simulations of LFs when the target size is fixed (the best choice for the $\delta t = 0.001$ was selected). Note that for better visual comparison of the PDFs their values were divided by a factor of 10 for $\delta t = 0.005$ and of 100 for $\delta t = 0.01$. Parameters: $\alpha = 1.5$, $K_\alpha = 1$, $x_0 = 1$, and $d = 0.014$.

moved towards longer t . No matter how small the target is chosen, the proper point-like target long-time scaling will be observed at some time scale. However, any simulation has a finite duration. Hence, it is reasonable to choose a target size which leads to the theoretical scaling within the time cutoff limit of the run. The set of best choices for other α used is listed in the main text.

Since the overshoots also depend on the time discretisation one has to adjust it as well. In figure G2 we show how the long time characteristics change with δt while keeping the target size $d = 0.014$ for $\alpha = 1.5$. The change of δt leads to deviations from the proper long-time behaviour of the first-hitting PDF. Importantly, the number of runs does not affect the exponent obtained by averaging over a fixed interval of time. However, the accuracy of defining of the exponents increases with the number of runs.

Appendix H. Shape of the Lévy walk propagator

The shape of the LW propagator discussed in section 4.2 is shown in figure H1.

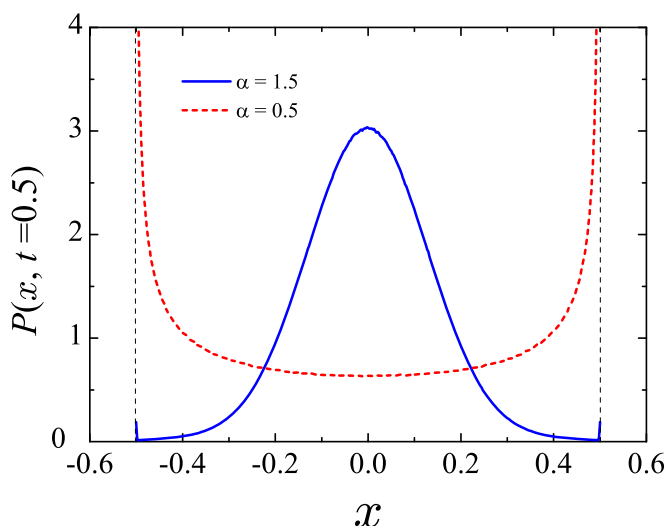


Figure H1. LW PDF for $\alpha = 0.5$ and $\alpha = 1.5$ at $t = 0.5$, for $v = 1$. For $\alpha = 0.5$ the PDF is U-shaped while for $\alpha = 1.5$ the PDF is bell-shaped. In both cases the horizon of the PDF is at $|x| = 0.5$, note the spikes at $|x| = 0.5$ for $\alpha = 1.5$.

ORCID iDs

Vladimir V Palyulin  <https://orcid.org/0000-0002-3047-6937>

Ralf Metzler  <https://orcid.org/0000-0002-6013-7020>

Rainer Klages  <https://orcid.org/0000-0003-3811-3070>

References

- [1] Redner S 2001 *A Guide to First Passage Processes* (Cambridge: Cambridge University Press)
- [2] Metzler R, Oshanin G and Redner S (ed) 2014 *First Passage Problems: Recent Advances* (Singapore: World Scientific)
- [3] Hughes B D 1995 *Random Walks and Random Environments, Vol 1: Random Walks* (Oxford: Oxford University Press)
- [4] Smoluchowski M V 1917 *Z. Phys. Chem.* **92** 129
- [5] Collins F C and Kimball G E 1949 *J. Colloid Sci.* **4** 425
- [6] Bunde A *et al* (ed) 2018 *Diffusive Spreading in Nature, Technology and Society* (Berlin: Springer)
- [7] Bénichou O and Voituriez R 2014 *Phys. Rep.* **539** 225
- [8] Bressloff P C and Newby J M 2013 *Rev. Mod. Phys.* **85** 135
- [9] Holcman D and Schuss Z 2014 *SIAM Rev.* **56** 213
- [10] Bénichou O, Chevalier C, Klafter J, Meyer B and Voituriez R 2010 *Nat. Chem.* **2** 472
- [11] Kolesov G, Wunderlich Z, Laikova O N, Gelfand M S and Mirny L A 2007 *Proc. Natl Acad. Sci. USA* **104** 13948
- [12] Pulkkinen O and Metzler R 2013 *Phys. Rev. Lett.* **110** 198101
- [13] Godec A and Metzler R 2016 *Phys. Rev. X* **6** 041037
- [14] Grebenkov D, Metzler R and Oshanin G 2018 *Commun. Chem.* **1** 96
- [15] Metzler R and Klafter J 2000 *Phys. Rep.* **339** 1
- [16] Metzler R and Klafter J 2004 *J. Phys. A: Math. Gen.* **37** R161
- [17] Klages R, Radons G and Sokolov I M (ed) 2008 *Anomalous Transport: Foundations and Applications* (New York: Wiley)
- [18] Höfling F and Franosch T 2013 *Rep. Prog. Phys.* **76** 046602
- [19] Metzler R, Jeon J-H, Cherstvy A G and Barkai E 2014 *Phys. Chem. Chem. Phys.* **16** 24128
- [20] Zaborudav V, Denisov S and Klafter J 2015 *Rev. Mod. Phys.* **87** 483
- [21] Siegle P, Goychuk I and Hänggi P 2010 *Phys. Rev. Lett.* **105** 100602
- [22] Richardson L F 1926 *Proc. R. Soc. A* **110** 709
- [23] Scher H and Montroll E W 1975 *Phys. Rev. B* **12** 2455
- [24] Brockmann D, Hufnagel L and Geisel T 2006 *Nature* **439** 462–5
- [25] Barthélemy P, Bertolotti J and Wiersma D S 2008 *Nature* **453** 495
- [26] Dieterich P, Klages R, Preuss R and Schwab A 2008 *Proc. Natl Acad. Sci. USA* **105** 459
- [27] Harris T H *et al* 2012 *Nature* **486** 545
- [28] Ariel G, Rabani A, Benisty S, Partridge J D, Harshey R M and Be'er A 2015 *Nat. Commun.* **6** 8396
- [29] Ariel G, Be'er A and Reynolds A 2017 *Phys. Rev. Lett.* **118** 228102
- [30] Barkai E, Garini Y and Metzler R 2012 *Phys. Tod.* **65** 29
- [31] Krapf D and Metzler R 2019 *Phys. Today* **72** 48
- [32] Nørregaard K, Metzler R, Ritter C M, Berg-Sørensen K and Oddershede L B 2017 *Chem. Rev.* **117** 4342
- [33] Metzler R, Jeon J H and Cherstvy A G 2016 *Biochim. Biophys. Acta* **1858** 2451
- [34] Mandelbrot B B and van Ness J W 1968 *SIAM Rev.* **10** 422
- [35] Molchan G M 1999 *Commun. Math. Phys.* **205** 97
- [36] Jeon J-H, Chechkin A V and Metzler R 2011 *Europhys. Lett.* **94** 20008
- [37] Sokolov I M 2003 *Phys. Rev. Lett.* **90** 080601

- [37] Chechkin A, Metzler R, Klafter J and Gonchar V Introduction to the theory of Lévy flights, in [17]
- [38] Metzler R, Chechkin A V and Klafter J 2009 Lévy statistics and anomalous transport: Lévy flights and subdiffusion *Encyclopedia of Complexity and Systems Science* ed R Mayers (New York: Springer)
- [39] Dubkov A A, Spagnolo B and Uchaikin V V 2008 *Intern. J. Bifurcation Chaos* **18** 2649
Dubkov A A and Spagnolo B 2005 *Fluct. Noise Lett.* **5** L267
- [40] Klafter J, Blumen A and Shlesinger M F 1987 *Phys. Rev. A* **35** 3081
- [41] Fogedby H C 1994 *Phys. Rev. E* **50** 1657
- [42] Shlesinger M F, Klafter J and Wong Y M 1982 *J. Stat. Phys.* **27** 499
- [43] Zumofen G and Klafter J 1993 *Phys. Rev. E* **47** 851
- [44] Denisov S, Zaburdaev V and Hänggi P 2012 *Phys. Rev. E* **85** 031148
- [45] Albers T and Radons G 2018 *Phys. Rev. Lett.* **120** 104501
- [46] Froemberg D and Barkai E 2013 *Phys. Rev. E* **87** 030104(R)
- [47] Froemberg D and Barkai E 2013 *Euro Phys. J. B* **86** 331
- [48] Godec A and Metzler R 2013 *Phys. Rev. Lett.* **110** 020603
- [49] Akimoto T 2012 *Phys. Rev. Lett.* **108** 164101
- [50] Froemberg D and Barkai E 2013 *Phys. Rev. E* **88** 024101
- [51] Godec A and Metzler R 2013 *Phys. Rev. E* **88** 012116
- [52] Metzler R, Barkai E and Klafter J 1999 *Europhys. Lett.* **46** 431
- [53] Kaminska A and Srokowski T 2017 *Phys. Rev. E* **96** 032105
Srokowski T 2017 *Phys. Rev. E* **95** 032133
- [54] Gardiner C 2009 *Stochastic Methods, A Handbook for the Natural and Social Sciences* (Berlin: Springer)
- [55] Koren T, Chechkin A V and Klafter J 2007 *Physica A* **379** 10
- [56] Koren T, Lomholt M A, Chechkin A V, Klafter J and Metzler R 2007 *Phys. Rev. Lett.* **99** 160602
- [57] Dybiec B, Gudowska-Nowak E, Barkai E and Dubkov A A 2017 *Phys. Rev. E* **95** 052102
- [58] Pavlyukevich I 2007 *J. Comput. Phys.* **226** 1830
Pavlyukevich I 2008 *Stochast. Process. Applic.* **118** 1071
- [59] Teuerle M, Żebrowski P and Magdziarz M 2012 *J. Phys. A: Math. Theor.* **45** 385002
- [60] Zaburdaev V, Fouxon I, Denisov S and Barkai E 2016 *Phys. Rev. Lett.* **117** 270601
- [61] Palyulin V V, Chechkin A V, Klages R and Metzler R 2016 *J. Phys. A: Math. Theor.* **49** 394002
- [62] Mandelbrot B B 1982 *The Fractal Geometry of Nature* (New York: Freeman)
- [63] Lomholt M A, Ambjörnsson T and Metzler R 2005 *Phys. Rev. Lett.* **85** 260603
Compare also Sokolov I M, Mai J and Blumen A 1999 *Phys. Rev. Lett.* **79** 857
- [64] Mantegna R N and Stanley H E 1994 *Phys. Rev. Lett.* **73** 2946
- [65] Koponen I 1995 *Phys. Rev. E* **52** 1197
- [66] Chechkin A V, Gonchar V Y, Klafter J and Metzler R 2005 *Phys. Rev. E* **72** 010101(R)
- [67] Klages R 2016 Search for food of birds, fish and insects *Diffusive Spreading in Nature, Technology and Society* ed A Bunde et al (Berlin: Springer)
- [68] Katori H, Schlipf S and Walther H 1997 *Phys. Rev. Lett.* **79** 2221
- [69] Geisel T and Thomae S 1984 *Phys. Rev. Lett.* **52** 1936
- [70] Geisel T, Nierwetberg J and Zacherl A 1985 *Phys. Rev. Lett.* **54** 616
- [71] Shlesinger M F and Klafter J 1985 *Phys. Rev. Lett.* **54** 2551
- [72] Shlesinger M F and Klafter J 1986 *On Growth and Form* ed H E Stanley (Dordrecht: Kluwer) pp 279–83
- [73] Viswanathan G M, Afanasyev V, Buldyrev S V, Murphy E J, Prince P A and Stanley H E 1996 *Nature* **381** 413
- [74] Edwards A M et al 2007 *Nature* **449** 1044
- [75] Humphries N E, Weimerskirch H, Queiroz N, Southall E J and Sims D W 2012 *Proc. Natl Acad. Sci. USA* **109** 7169
- [76] Viswanathan G M, Buldyrev S V, Havlin S, da Luz M G E, Raposo E P and Stanley H E 1999 *Nature* **401** 911
- [77] Viswanathan G M, da Luz M G E, Raposo E P and Stanley H E 2011 *The Physics of Foraging* (Cambridge: Cambridge University Press)
- [78] Bénichou O, Loverdo C, Moreau M and Voituriez R 2011 *Rev. Mod. Phys.* **83** 81
- [79] Pyke G H 2015 *Meth. Ecol. Evol.* **6** 16
- [80] Palyulin V V, Chechkin A V and Metzler R 2014 *Proc. Natl Acad. Sci. USA* **111** 2931
- [81] Palyulin V V, Chechkin A V and Metzler R 2014 *J. Stat. Mech.* **P11031**
- [82] Palyulin V V, Mantsevich V N, Klages R, Metzler R and Chechkin A V 2017 *Eur. Phys. J. B* **90** 170
- [83] Bénichou O, Loverdo C, Moreau M and Voituriez R 2006 *Phys. Rev. E* **74** 020102(R)
- [84] Oshanin G, Lindenberg K, Wio H S and Burlatsky S 2009 *J. Phys. A: Math. Theor.* **42** 434008
- [85] Lomholt M A, Koren T, Metzler R and Klafter J 2008 *Proc. Natl Acad. Sci. U.S.A.* **105** 11055
- [86] Kuśmiercz Ł and Gudowska-Nowak E 2015 *Phys. Rev. E* **92** 052127
- [87] Benhamou S 2007 *Ecology* **88** 1962–9
- [88] James A, Pitchford J W and Plank M J 2009 *Bull. Math. Biol.* **72** 896
- [89] Siegert A J F 1951 *Phys. Rev.* **81** 4
- [90] He J 2009 *Appl. Math. Mech.—English Ed.* **30** 255–62
- [91] Shinozuka M and Wu W-F 1988 On the first passage problem and its application to earthquake engineering *Proc. 9th World Conf. on Earthquake Engineering* vol VIII (Tokyo-Kyoto, Japan, 2–9 August) pp 767–72
- [92] Gerstein G L and Mandelbrot B B 1964 *Biophys. J.* **4** 41
- [93] Dybiec B and Gudowska-Nowak E 2009 *J. Stat. Mech.* **P05004**
- [94] Kearney M J and Majumdar S N 2005 *J. Phys. A: Math. Gen.* **38** 4097
- [95] Eichner J F, Kantelhardt J W, Bunde A and Havlin S 2006 *Phys. Rev. E* **73** 016130
- [96] Kindermann F, Hohmann M, Lausch T, Mayer D, Schmidt F and Widera A 2017 *Phys. Rev. E* **96** 012130
- [97] Mandelbrot B 1963 *J. Business* **36** 394
- [98] Chechkin A V, Metzler R, Gonchar V Y, Klafter J and Tanatarov L V 2003 *J. Phys. A: Math. Gen.* **36** L537
- [99] Majumdar S N, Mounaix P and Schehr G 2017 *J. Phys. A: Math. Theor.* **50** 465002
- [100] Chambers J M, Mallows C L and Stuck B W 1976 *J. Am. Stat. Assoc.* **71** 340
- [101] Augello G, Valenti D and Spagnolo B 2010 *Euro. Phys. J. B* **78** 225
- [102] Lee M-L T and Whitmore G A 1993 *J. Appl. Prob.* **30** 302

- [103] Korabel N and Barkai E 2011 *J. Stat. Mech.* **P05022**
- [104] Metzler R and Klafter J 2000 *Physica A* **278** 107
- [105] Artuso R, Cristadoro G, Esposti M D and Knight G 2014 *Phys. Rev. E* **89** 052111
- [106] Campos D, Abad E, Méndez V, Yuste S B and Lindenberg K 2015 *Phys. Rev. E* **91** 052115
- [107] Dybiec B, Gudowska-Nowak E and Chechkin A 2016 *J. Phys. A: Math. Theor.* **49** 504001
- [108] Janakiraman D 2017 *Phys. Rev. E* **95** 012154
- [109] Erdélyi A (ed) 1981 *Higher Transcendental Functions, vol III, Bateman Manuscript Project* (Malabar, FL: Krieger)
- [110] Lenz F, Ings T C, Chittka L, Chechkin A V and Klages R 2012 *Phys. Rev. Lett.* **108** 098103
- [111] Kusmierz L, Majumdar S N, Sabhapandit S and Schehr G 2014 *Phys. Rev. Lett.* **113** 220602
- Kusmierz L and Gudowska-Nowak E 2015 *Phys. Rev. E* **92** 052127
- [112] Dieterich P et al 2018 Asymmetric anomalous diffusion in neutrophil chemotaxis (submitted)
- [113] Chechkin A V, Gonchar V Y, Klafter J, Metzler R and Tanatarov L V 2002 *Chem. Phys.* **284** 233
- Chechkin A V, Klafter J, Gonchar V Y, Metzler R and Tanatarov L V 2003 *Phys. Rev. E* **67** 010102(R)
- Chechkin A V, Gonchar V Y, Klafter J, Metzler R and Tanatarov L V 2004 *J. Stat. Phys.* **115** 1505
- Dubkov A A and Spagnolo B 2013 *Euro. Phys. J. Spec. Top.* **216** 31
- Dubkov A and Spagnolo B 2007 *Acta Phys. Polon. B* **38** 1745
- Kharcheva A A, Dubkov A A, Dybiec B, Spagnolo B and Valenti D 2016 *J. Stat. Mech.* **054039**
- Dybiec B, Capala K, Chechkin A and Metzler R 2019 *J. Phys. A: Math. Theor.* **52** 015001
- [114] Chechkin A V, Gonchar V Y, Klafter J and Metzler R 2005 *Europhys. Lett.* **72** 348
- Chechkin A V, Sliusarenko O Y, Metzler R and Klafter J 2007 *Phys. Rev. E* **75** 041101
- Dubkov A A, La Cognata A and Spagnolo B 2009 *J. Stat. Mech.* **P01002**
- [115] Dubkov A A and Spagnolo B 2008 *Euro. Phys. J. B* **65** 361
- Lisowski B, Valenti D, Spagnolo B, Bier M and Gudowska-Nowak E 2015 *Phys. Rev. E* **91** 042713
- La Cognata A, Valenti D, Dubkov A A and Spagnolo B 2010 *Phys. Rev. E* **82** 011121
- [116] Spagnolo B, Valenti D, Guarcello C, Carollo A, Persano Adorno D, Spezia S, Pizzolato N and Paola B Di 2015 *Chaos Solitons Fractals* **81** 412
- Guarcello C, Valenti D, Carollo A and Spagnolo B 2016 *J. Stat. Mech.* **054012**
- Spagnolo B, Guarcello C, Magazzu L, Carollo A, Persano Adorno D and Valenti D 2017 *Entropy* **19** 20
- Guarcello C, Valenti D, Spagnolo B, Pierro V and Filatrella G 2017 *Nanotechnology* **28** 134001
- Guarcello C, Valenti D, Spagnolo B, Pierro V and Filatrella G 2019 *Phys. Rev. Appl.* **11** 044078
- [117] Sposini V, Chechkin A V and Metzler R 2019 *J. Phys. A: Math. Theor.* **52** 04LT01
- Lanoiselée Y, Moutal N and Grebenkov D S 2018 *Nat. Commun.* **9** 4398
- Chechkin A V, Seno F, Metzler R and Sokolov I M 2017 *Phys. Rev. X* **7** 021002
- [118] Oshanin G, Vasilyev O, Krapivsky P L and Klafter J 2009 *Proc. Natl Acad. Sci. USA* **106** 13696
- Schwarzl M, Godec A, Oshanin G and Metzler R 2016 *J. Phys. A: Math. Theor.* **49** 225601
- [119] Prudnikov A P, Brychkov Y A and Marichev O I 1990 *Integrals and Series* (New York: Gordon and Breach Science)
- [120] Abramowitz M and Stegun I 1972 *Handbook of Mathematical Functions with Formulas, Graphs, and Mathematical Tables* (New York: Dover)
- [121] Mathai A M, Saxena R K and Haubold H J 2010 *The H-Function Theory and Applications* (New York: Springer)
- [122] Podlubny I 1998 *Fractional Differential Equations* (New York: Academic)
- [123] Malakhov A N 1968 *Fluctuations in Self-Oscillating Systems [in Russian]* (Moscow: Nauka)